REPORT DOCUMENTATION PAGE

Form Approved OMB NO. 0704-0188

1. REPORT DATE (DD-MM-YYYY)	2. REPORT TYPE	3. DATES COVERED (From - To)
21-11-2009	Final Report	1-Oct-2005 - 31-Mar-2009

4. TITLE AND SUBTITLE
Evolution and Survival of Quantum Entanglement

5a. CONTRACT NUMBER
W911NF-05-1-0543

5b. GRANT NUMBER

5c. PROGRAM ELEMENT NUMBER
611102

6. AUTHORS
J.H. Eberly

5d. PROJECT NUMBER

5e. TASK NUMBER

5f. WORK UNIT NUMBER

7. PERFORMING ORGANIZATION NAMES AND ADDRESSES
University of Rochester
Office of Research & Project Administration
518 Hylan Bldg., River Campus Box 270140
Rochester, NY 14627 -

8. PERFORMING ORGANIZATION REPORT NUMBER

9. SPONSORING/MONITORING AGENCY NAME(S) AND ADDRESS(ES)
U.S. Army Research Office
P.O. Box 12211
Research Triangle Park, NC 27709-2211

10. SPONSOR/MONITOR'S ACRONYM(S)
ARO

11. SPONSOR/MONITOR'S REPORT NUMBER(S)
48422-PH.1

12. DISTRIBUTION AVAILABILITY STATEMENT
Approved for Public Release; Distribution Unlimited

13. SUPPLEMENTARY NOTES
The views, opinions and/or findings contained in this report are those of the author(s) and should not contrued as an official Department of the Army position, policy or decision, unless so designated by other documentation.

14. ABSTRACT
The program of the grant (evolution and survival of quantum entanglement) was advanced by extending to open-system relevance an important lead reported earlier (provided by Jaynes-Cummings closed-system modelling). We report success in tracking the movement of quantum entanglement. Reversals of the entanglement sudden death (ESD) effect are now also open to study in the case of "revival" effects in coherent-state quantum fields. A new finding is the discovery of a way to hide entanglement completely (reducing concurrence to

15. SUBJECT TERMS
entanglement, quantum memory, information transfer, non-local memory evolution, open system, coherent state

16. SECURITY CLASSIFICATION OF: a. REPORT	b. ABSTRACT	c. THIS PAGE	17. LIMITATION OF ABSTRACT	15. NUMBER OF PAGES	19a. NAME OF RESPONSIBLE PERSON
UU	UU	UU	UU		Joseph Eberly
					19b. TELEPHONE NUMBER
					585-273-2484

Report Title

Evolution and Survival of Quantum Entanglement

ABSTRACT

The program of the grant (evolution and survival of quantum entanglement) was advanced by extending to open-system relevance an important lead reported earlier (provided by Jaynes-Cummings closed-system modelling). We report success in tracking the movement of quantum entanglement. Reversals of the entanglement sudden death (ESD) effect are now also open to study in the case of "revival" effects in coherent-state quantum fields. A new finding is the discovery of a way to hide entanglement completely (reducing concurrence to effectively zero values) for extended periods, but then recover it with manageable loss at later times on a managed schedule. An extended account of work done, with accompanying papers, is attached.

List of papers submitted or published that acknowledge ARO support during this reporting period. List the papers, including journal references, in the following categories:

(a) Papers published in peer-reviewed journals (N/A for none)

T. Yu and J.H. Eberly
Entanglement Evolution in a Non-Markovian Environment
Optics Comm. (in press, 2009).

T. Yu and J.H. Eberly
Entanglement Sudden Death
Science {323}, 598 (2009).

Number of Papers published in peer-reviewed journals: 2.00

(b) Papers published in non-peer-reviewed journals or in conference proceedings (N/A for none)

Number of Papers published in non peer-reviewed journals: 0.00

(c) Presentations

- invited talk, ECE Colloquium
"Quantum Mechanics and Weird Quantum Optics"
U. Minnesota Sept. 18, 2008
Minneapolis MN

****
- invited talk, Z. Fried Mem. Lect.
"Quantum Weirdness and Clauser's Interferometer"
U. Mass. - Lowell, Nov. 19, 2008
Lowell MA

****
- invited Plenary Lecture
Workshop on Metamaterials / Meta-In Workshop
"Control of Radiative Interactions and Quantum Entanglement"
Univ. Hyderabad, Dec. 18-20, 2008
Hyderabad INDIA

****
- Joint Physics Appl. Physics Colloquium
"The Unnatural Death of Quantum Entanglement"
UC Davis, March 9, 2009
Davis CA

****
- inv. talk
"Interpreting Quantum Information with the Clauser-Aspect Interferometer"
APS - NY State Section, April 17-18, 2009
Rochester NY

****

Number of Presentations: 5.00

Non Peer-Reviewed Conference Proceeding publications (other than abstracts):

Number of Non Peer-Reviewed Conference Proceeding publications (other than abstracts): 0

Peer-Reviewed Conference Proceeding publications (other than abstracts):

Number of Peer-Reviewed Conference Proceeding publications (other than abstracts): 0

(d) Manuscripts

M. Yonac and J.H. Eberly
"Evolution of Long-Time Non-Interacting Quantum Entanglement"
submitted to Physical Review A

Number of Manuscripts: 1.00

Number of Inventions:

Graduate Students

NAME	PERCENT_SUPPORTED
Muhammed Yonac	0.25
Xiao-Feng Qian	0.50
FTE Equivalent:	**0.75**
Total Number:	**2**

Names of Post Doctorates

NAME	PERCENT_SUPPORTED
FTE Equivalent:	
Total Number:	

Names of Faculty Supported

NAME	PERCENT_SUPPORTED	National Academy Member
Joseph Eberly	0.10	No
FTE Equivalent:	**0.10**	
Total Number:	**1**	

Names of Under Graduate students supported

NAME	PERCENT_SUPPORTED
FTE Equivalent:	
Total Number:	

Student Metrics

This section only applies to graduating undergraduates supported by this agreement in this reporting period

The number of undergraduates funded by this agreement who graduated during this period: 0.00

The number of undergraduates funded by this agreement who graduated during this period with a degree in science, mathematics, engineering, or technology fields:...... 0.00

The number of undergraduates funded by your agreement who graduated during this period and will continue to pursue a graduate or Ph.D. degree in science, mathematics, engineering, or technology fields:...... 0.00

Number of graduating undergraduates who achieved a 3.5 GPA to 4.0 (4.0 max scale):...... 0.00

Number of graduating undergraduates funded by a DoD funded Center of Excellence grant for Education, Research and Engineering:...... 0.00

The number of undergraduates funded by your agreement who graduated during this period and intend to work for the Department of Defense 0.00

The number of undergraduates funded by your agreement who graduated during this period and will receive scholarships or fellowships for further studies in science, mathematics, engineering or technology fields:...... 0.00

Names of Personnel receiving masters degrees

NAME
Total Number:

Names of personnel receiving PHDs

NAME	
Muhammed Yonac	
Total Number:	**1**

Names of other research staff

NAME	PERCENT_SUPPORTED
FTE Equivalent:	
Total Number:	

Sub Contractors (DD882)

Inventions (DD882)

Attachment to Final Report - 48422PH - Evolution and Survival of Quantum Entanglement, J.H. Eberly, PI

1. Foreword - none

2. ToC - none needed

3. List of Appendices -

    A. pdf of review published: Science {323}, 598 (2009)
    B. pdf of paper submitted: Phys. Rev. A (submitted)
    C. pdf of paper accepted: Optics Commun. (in press, 2009)

4. Statement of problem studied -

The behavior of quantum entanglement under various types of environmental noise was studied. Both the nature of its evolution in time and the nature of its survival were examined. Attention was confined to pure non-local entanglement, appropriate to quantum memory registers, for which preservation of entanglement is important.

5. Summary of most important results - three results stand out:

A. The state of knowledge was substantially advanced by recognizing the unexpected behavior of quantum decoherence when attacking entangled qubits. This can be finished non-analytically, i.e., in a finite time, in contrast to its smooth exponential behavior when attacking local coherences (T1 and T2 types). This was reviewed by invitation in Science (see App. A).

B. We also extend an important lead reported earlier (provided by Jaynes-Cummings closed-system modelling) to open systems, with which we reported success in tracking the movement of quantum entanglement (see App. B).

C. We also showed that the most common model of non-Markov noise could be studied fully analytically. This will lead to improvement in methods for dealing with the effect on quantum entanglement of real-life noise sources.

6. Bibliography - see Appendices

7. Appendices -

App. A, Science {323}, 598 (2009);

App. B, Phys. Rev. A (submitted);

App. C, Optics Commun. (in press, 2009).

Science AAAS

Sudden Death of Entanglement

Ting Yu, *et al.*

Science **323**, 598 (2009);
DOI: 10.1126/science.1167343

Sudden Death of Entanglement

Ting Yu[1]* and J. H. Eberly[2]*

A new development in the dynamical behavior of elementary quantum systems is the surprising discovery that correlation between two quantum units of information called qubits can be degraded by environmental noise in a way not seen previously in studies of dissipation. This new route for dissipation attacks quantum entanglement, the essential resource for quantum information as well as the central feature in the Einstein-Podolsky-Rosen so-called paradox and in discussions of the fate of Schrödinger's cat. The effect has been labeled ESD, which stands for early-stage disentanglement or, more frequently, entanglement sudden death. We review recent progress in studies focused on this phenomenon.

Quantum entanglement is a special type of correlation that can be shared only among quantum systems. It has been the focus of foundational discussions of quantum mechanics since the time of Schrödinger (who gave it its name) and the famous EPR paper of Einstein, Podolsky, and Rosen (*1*, *2*). The degree of correlation available with entanglement is predicted to be stronger as well as qualitatively different compared with that of any other known type of correlation. Entanglement may also be highly nonlocal—e.g., shared among pairs of atoms, photons, electrons, etc., even though they may be remotely located and not interacting with each other. These features have recently promoted the study of entanglement as a resource that we believe will eventually find use in new approaches to both computation and communication, for example, by improving previous limits on speed and security, in some cases dramatically (*3*, *4*).

Quantum and classical correlations alike always decay as a result of noisy backgrounds and decorrelating agents that reside in ambient environments (*5*), so the degradation of entanglement shared by two or more parties is unavoidable (*6*–*9*). The background agents with which we are concerned have extremely short (effectively zero) internal correlation times themselves, and their action leads to the familiar law mandating that after each successive half-life of decay, there is still half of the prior quantity remaining, so that a diminishing fraction always remains.

However, a theoretical treatment of two-atom spontaneous emission (*10*) shows that quantum entanglement does not always obey the half-life law. Earlier studies of two-party entanglement in different model forms also pointed to this fact (*11*–*15*). The term now used, entanglement sudden death (ESD, also called early-stage disentanglement), refers to the fact that even a very weakly dissipative environment can degrade the specifically quantum portion of the correlation to zero in a finite time (Fig. 1), rather than by successive halves. We will use the term "decoherence" to refer to the loss of quantum correlation, i.e., loss of entanglement.

This finite-time dissipation is a new form of decay (*16*), predicted to attack only quantum entanglement, and not previously encountered in the dissipation of other physical correlations. It has been found in numerous theoretical examinations to occur in a wide variety of entanglements involving pairs of atomic, photonic, and spin qubits, continuous Gaussian states, and subsets of multiple qubits and spin chains (*17*). ESD has already been detected in the laboratory in two different contexts (*18*, *19*), confirming its experimental reality and supporting its universal relevance (*20*). However, there is still no deep understanding of sudden death dynamics, and so far there is no generic preventive measure.

How Does Entanglement Decay?

An example of an ESD event is provided by the weakly dissipative process of spontaneous emission, if the dissipation is "shared" by two atoms (Fig. 1). To describe this we need a suitable notation.

The pair of states for each atom, sometimes labeled (+) and (−) or (1) and (0), are quantum analogs of "bits" of classical information, and hence such atoms (or any quantum systems with just two states) are called quantum bits or "qubits." Unlike classical bits, the states of the atoms have the quantum ability to exist in both states at the same time. This is the kind of superposition used by Schrödinger when he introduced his famous cat, neither dead nor alive but both, in which case the state of his cat is conveniently coded by the bracket (+ ⇔ −), to indicate equal simultaneous presence of the opposite + and − conditions.

This bracket notation can be extended to show entanglement. Suppose we have two opposing conditions for two cats, one large and one small, and either waking (W) or sleeping (S). Entanglement of idealized cats could be denoted with a bracket such as [(*Ws*) ⇔ (*Sw*)], where we have chosen large and small letters to distinguish a big cat from a little cat. The bracket would signal via the term (*Ws*) that the big cat is awake and the little cat is sleeping, but the other term (*Sw*) signals that the opposite is also true, that the big cat is sleeping and the little cat is awake.

One can see the essence of entanglement here: If we learn that the big cat is awake, the (*Sw*) term must be discarded as incompatible with what we learned previously, and so the two-cat state reduces to (*Ws*). We immediately conclude that the little cat is sleeping. Thus, knowledge of the state of one of the cats conveys information about the other (*21*). The brackets are symbols of information about the cats' states, and do not belong to one cat or the other. The brackets belong to the reader, who can make predictions based on the information the brackets convey. The same is true of all quantum mechanical wave functions.

Entanglement can be more complicated, even for idealized cats. In such cases, a two-party joint state must be represented not by a bracket as above, but by a matrix, called a density matrix and denoted ρ in quantum mechanics [see (*22*) and Eq. S3]. When exposed to environmental noise, the density matrix ρ will change in time, becoming degraded, and the accompanying change in entanglement can be tracked with a quantum mechanical variable called concurrence (*23*), which is written for qubits such as the atoms *A* and *B* in Fig. 1 as

$$C(\rho) = \max[0, Q(t)] \tag{1}$$

where $Q(t)$ is an auxilliary variable defined in terms of entanglement of formation, as given explicitly in Eq. S4. $C = 0$ means no entanglement and is achieved whenever $Q(t) \leq 0$, while for

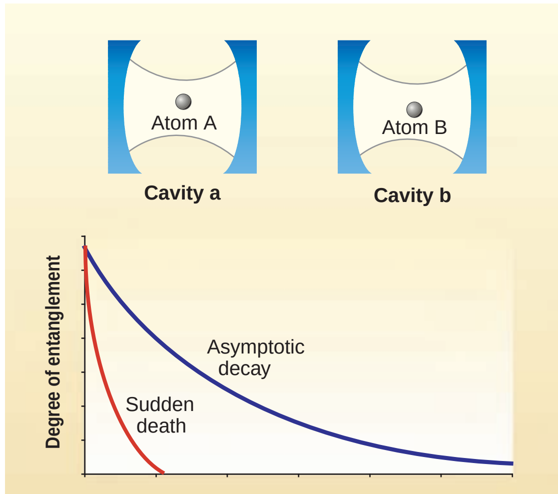

Fig. 1. Curves show ESD as one of two routes for relaxation of the entanglement, via concurrence $C(\rho)$, of qubits *A* and *B* that are located in separate overdamped cavities.

[1]Department of Physics and Engineering Physics, Stevens Institute of Technology, Hoboken, NJ 07030–5991, USA. [2]Rochester Theory Center and Department of Physics and Astronomy, University of Rochester, Rochester, NY 14627–0171, USA.

*E-mail: ting.yu@stevens.edu (T.Y.), eberly@pas.rochester.edu (J.H.E.)

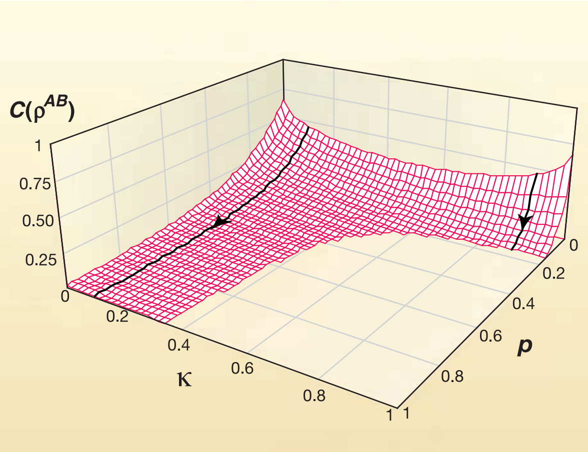

Fig. 2. Atom-atom entanglement is plotted as a function of time for κ values in the range 0 to 1. [Adapted from (*20*)] For all values of κ less than ⅓, the half-life rule is obeyed, but for κ between ⅓ and 1, it is not. For those values, the curves show ESD, i.e., becoming zero in a finite time and remaining zero thereafter. The two curves marked with arrows are similar to the curves in Fig. 1. Time is represented by $p = 1 - \exp(-\Gamma t)$.

maximally entangled states $C = 1$, and C is limited to the range $1 \geq C \geq 0$.

In the case of spontaneous emission there is no environment at all, except for the vacuum. The vacuum can still have a noisy degrading effect through its quantum fluctuations, which cannot be avoided, so both atoms in Fig. 1 must eventually lose their excitation and come to their ground states with the rate Γ. Then their state is simply (−−), a completely disentangled situation because learning that the state of one atom is (−) does not change our information about the other, also (−). Thus, disentanglement is the eventual fate of the pair.

The question is, how quickly do they meet their fate? For the initial density matrix shown in Eq. S5, the answer is supplied by the surface graphed in Fig. 2, which shows possible pathways for entanglement dissipation as a function of time. The κ axis shows that the time evolution of entanglement depends on the value of the parameter that encodes the initial probability for the two atoms to be in the doubly excited state (++). The two extreme concurrence curves for κ = 1 and κ = 0 are the ones already shown in Fig. 1.

The sudden death behavior shown in the right highlighted curve of Fig. 2 is a new feature for physical dissipation (*16*, *20*) and is induced by classical as well as quantum noises (*24*). It is counterintuitive, based on all previous single-atom experience, because spontaneous emission is a process that obeys the half-life rule rigorously for individual atoms. But it turns out that the two-qubit correlation does not follow the one-qubit pattern. That is, the sudden death does not come from a shorter half-life; the entangled joint correlation does not even have the half-life property.

As reported in (*18*), the first experimental confirmation of ESD was made with an all-optical approach focusing on photonic polarization. It was achieved by the tomographic reconstruction of $\rho(t)$, and from it the $Q(t)$ variable, and thus the concurrence $C(\rho)$. In the experiment, both amplitude and phase noises that can degrade entanglement were realized by combining beam splitters and mirrors.

Can Sudden Death Be Avoided or Delayed?

The issue of how to avoid ESD-type decorrelation in a realistic physical system is incompletely resolved at this time. A number of methods are known to provide protection against previously known types of decorrelation (*3*). Some methods have classical analogs in information theory. One engages appropriately designed redundancy and is known as quantum error correction. Another relies on using a symmetry that can isolate entanglement from noise, effectively providing a decoherence-free subspace to manage qubit evolution.

Error correction is most useful when the disturbing noise is below some threshold (*25*). In practice error correction can be complicated, because a noisy channel is a dynamical process and its physical features are often not fully understood or predictable. An example is atmospheric turbulence during open-air communication. Another issue is the cost associated with providing redundancy. Additionally, it has been reported that some quantum error correction algorithms could actually promote rather than mitigate ESD (*26*). Symmetries that avoid decoherence by providing isolation from noise during evolution (*27*) have also been examined as a way to postpone or avoid ESD, but knowledge of the noise to be combatted appears unlikely to be available because qubits remote from each other would rarely share either symmetry properties or noise descriptions.

Other methods considered use dynamic manipulation such as mode modulation (*28*) or the quantum Zeno effect (*29*), which can be regarded as extensions of the so-called bang-bang method (*30*). Another proposal is to use feedback control (*31*) to prevent ESD and other decoherence effects in the presence of hostile noise. None of these methods is perfect, but they can be more effective if designed for specific noise avoidance.

Does the Number of Noises Matter?

Nonlocal entanglement raises the issue of ESD triggered by different noise processes and can refer to more than one noise source acting together on colocated entangled qubits, or to independent noise sources acting separately on remotely located members of a qubit pair. The rate of dissipation in the presence of several noise sources is normally the sum of the individual dissipation rates. More explicitly, if decay rates Γ_1 and Γ_2 come from the action of two distinct weak noises, then when the two noises are applied together to a physical system, the resulting relaxation rate is simply given by the sum of the separate rates: $\Gamma_1 + \Gamma_2$.

However, such a long-standing result does not hold for entanglement decay. This was discovered (*16*) by examining entanglement evolution of a set of X-form mixed-state matrices (Eq. S3) with $d = 0$, where d is the probability that both qubits are in their ground states. Straightforward calculations for the entire class are shown by the diagrams in Fig. 3, illustrating two qubits exposed together to amplitude noise as well as phase noise. The top two time-dependent curves show that the application of either noise separately allows long-running entanglement decay of the half-life type (no ESD). By contrast, the bottom curve reaches zero in a finite time. That is, the combined effect of the two noises causes ESD. The caption explains the colored squares. This illustrates the "supervulnerability" of paired-qubit entanglement when attacked by different independent noises. This result is universal in the sense that it continues to hold (*16*) even if the two noises attack one of the qubits but not the other, and also if each of the two qubits is remotely attacked by just one of the noises.

Is There an "Anti-ESD" or Rebirth Effect?

Special circumstances are needed to see "anti-ESD," the creation or rebirth of entanglement

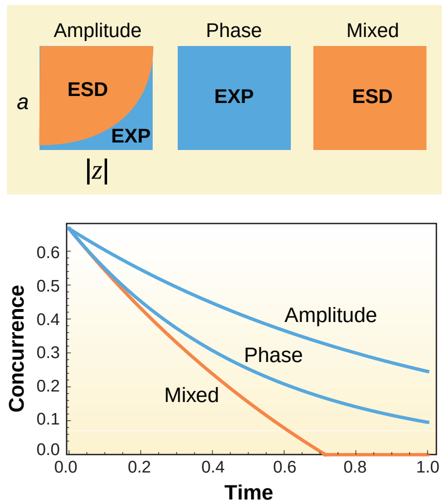

Fig. 3. The top two time-dependent curves show exponential (smooth half-life type) decay of concurrence for a qubit pair exposed to phase noise and to amplitude noise, respectively. The bottom curve shows nonsmooth decay, i.e., ESD occurs for the qubit pair when both noises are acting together. The color-coded squares apply to any two-party X matrix (Eq. S3) having $d = 0$. They present the predicted results for the entire accessible physical domain, which means throughout $1 \geq a \geq 0$ and $1 \geq |z| \geq 0$. The blue zones labeled EXP designate domains where smooth exponential (half-life type) evolution occurs, and the orange zones show where ESD occurs. The left and middle squares apply when amplitude and phase noises are applied separately, and have smooth decay regions, while the orange square at right shows that sudden death is universal in the entire region for any X matrix (Eq. S3).

from disentangled states. By imposing the right interactions almost anything can be made to happen, but we are concerned with evolution of joint information in a pure sense and focus on two-party entanglement that evolves without mutual interaction or communication.

The same two-atom situation shown in Fig. 1 can be made relevant to anti-ESD. In solving for the surface of solutions plotted in Fig. 2, the cavities were taken as fully overdamped, so that any photon emitted by either atom was irreversibly absorbed by the walls, but they could also be treated as undamped mirror-like cavities, such as used in the Jaynes-Cummings (JC) model for light-atom interactions (*32*). This situation produces a periodic sequence of perfect rebirths of atom *AB* entanglement (*33*, *34*). An early mathematical model of two-qubit evolution (*11*) can be interpreted as treating an underdamped cavity and also shows rebirths.

The panels in the top row of Fig. 4 show rebirth scenarios. They occur for states that are initially of the cat type, such that both atoms are excited and both are un-excited at the same time. The cat-type bracket for them is

$$\Phi_\alpha = [(++)\cos\alpha \Leftrightarrow (--)\sin\alpha] \qquad (2)$$

where different values of sine and cosine produce the different curves in the figure (*35*).

Starting from the photon vacuum state in each cavity, the JC-type evolution will permit only zero or one photon to reside in each cavity at any later time, so each of the two modes is a two-state system (a qubit), and counting the two atoms there are now four qubits on hand. This provides six concurrences that can be computed: C^{AB}, C^{ab}, C^{Ab}, C^{aB}, C^{Aa}, and C^{Bb}, where the capital letters identify atoms and the small letters identify the photons in cavity modes *a* or *b*. Concurrence is defined only for pairs of qubits, not quartets of them, so the label C^{AB} implies that the *a* and *b* degrees of freedom are not available to observation and have been ignored (technically, have been traced out), and for photon concurrence C^{ab} the atomic *A* and *B* properties are traced out, and so on.

This idealized model provides a convenient framework to analyze entanglement in a simplified but still multi-qubit framework. As shown in the top half of Fig. 4, ESD takes place for atom concurrence (in the left panel, almost all C^{AB} curves reach zero and remain zero for finite times). However, in the right panel, the photon concurrence C^{ab} behaves in a manner opposite to that of C^{AB}, showing anti-ESD. That is, initially C^{ab} is zero, but it immediately begins to grow. The photons jointly experience entanglement "sudden birth," but this is followed by ESD a half cycle later. All of this occurs via pure "informatics," i.e., without energy exchange or other interaction between the sites.

The reason for the rebirths is obvious—the photons emitted cannot really get lost among the few joint states available. If a larger number of cavity modes would be provided, a longer time would be needed for a rebirth to be complete, and as a limiting case, the cavities producing the curves in Fig. 2 have an infinite number of modes, so the lost quantum correlation cannot be reborn in any finite time. If there are enough states available in one mode, as is the case for coherent-state mode preparation, then ESD and true long-time revivals are also predicted (*36*).

What Are the Future Prospects?

Quantum memory banks. Clearly, ESD can be largely ignored, to a first approximation, when desirable quantum operations can be manipulated at sufficiently high speed. The key goal of memory is opposite to that of speed, i.e., to preserve quantum state features semi-indefinitely. Quantum memory networks will be sensitive to the consequences if ESD occurs. ESD will probably have to be taken into account if practical versions of quantum memories are built to operate in mixed-state configurations.

Disentanglement control. Over a given noisy channel, it appears that some entangled states may be more robust against the influence of noise than others. To control decoherence optimally, it will be useful to learn how to identify the robust states separately from the fragile ones. Control issues also include the use of external fields to manipulate qubit states (*37*) as in gate operations, to create transient decoherence-free subspaces, as mentioned already. A qualitatively different route to combat decoherence specifically of the ESD type is illustrated in Fig. 2. Two evolution tracks are highlighted to show that for qubits prepared with the same value of initial entanglement, their concurrences may evolve very differently. In that illustration, the right track is subject to ESD, while the left one is not. Decoherence per se is not avoided, because the non-ESD track shows steady dissipation, but it always remains finite. Other examples of this are known, and in some cases a purely local operation (i.e., a manipulation of only one of the two entangled qubits) can be undertaken to change the state matrix ρ without changing its degree of entanglement, but in a way that switches the evolution trajectory from ESD to non-ESD (*38*), effectively putting it on a half-life track as in the figure. Similar studies (*39*) have examined the effect of local operations at intermediate stages of evolution. Use of this method requires detailed knowledge of the state matrix ρ, which may not be practical, particularly at times late in the evolution.

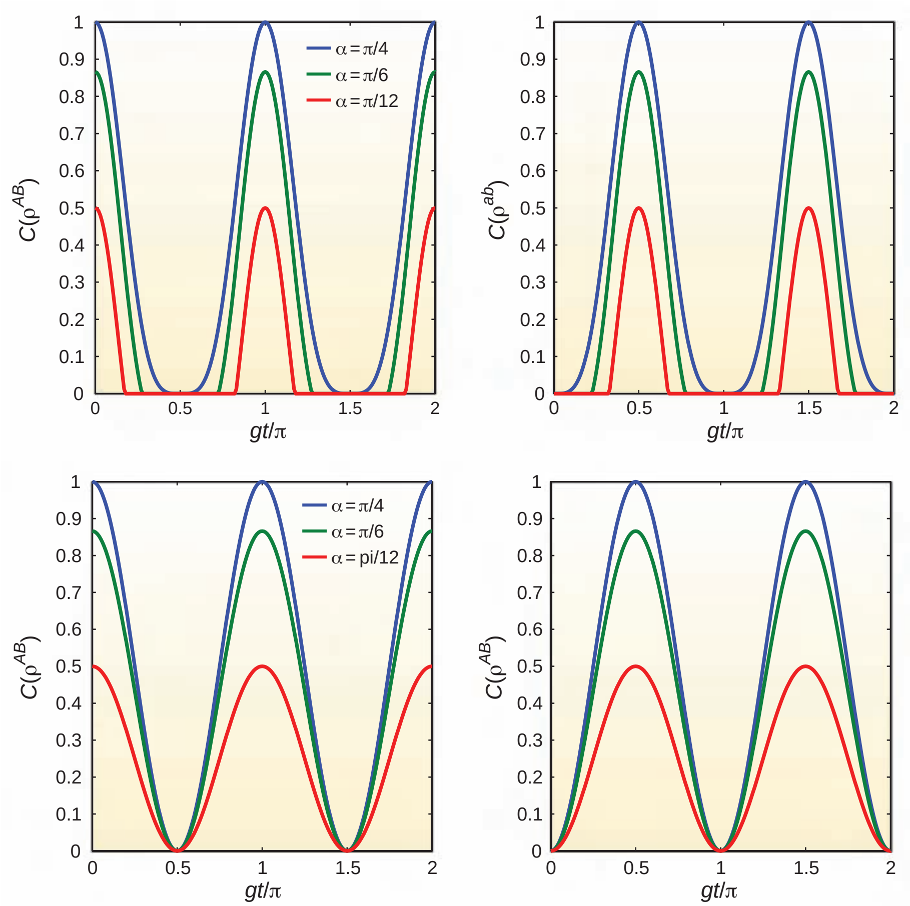

Fig. 4. Entanglement birth, death, and rebirth. [Adapted from (*35*)] In the bottom pair of panels the rise and fall of *AB* entanglement is exactly compensated by the fall and rise of *ab* entanglement. This is not the case in the top pair of panels, but a more subtle form of compensation still occurs, as reported in (*35*). It involves not concurrence but the auxiliary variable *Q*(*t*) defined in Eqs. 1 and S4.

Entanglement invariants. Entanglement flow in small reservoirs has led to the recent discovery of entanglement "invariants" (*35*) by inspection of the curves in the bottom row of Fig. 4, which repeats the top row except that a slightly different cat state is used for the atoms initially:

$$\Psi_\alpha = [(+-)\cos\alpha \Leftrightarrow (-+)\sin\alpha] \quad (3)$$

In the bottom left panel of Fig. 4, it appears that each *AB* atomic concurrence curve is compensated at all times by the corresponding *ab* photonic concurrence curve in the right panel, one going up as the other falls.

In fact, exact compensation can be confirmed analytically (*35*), but one notes that the same behavior does not appear in the top-row curves in Fig. 4, where there is no perfect compensation of *ab* for *AB*. For example, it is easy to see that the *AB* and *ab* red curves can be zero at the same time. A natural question is, where does the missing information go in that case? Because the two-site JC model is unitary, preservation of all four-qubit information is guaranteed, so it should be located "somewhere." Careful examination shows that concurrence is not conserved, but rather $Q(t)$ is conserved, spread among all six different types in that case (*35*).

This identification of four-particle memory flow channels is unusual and clearly deserves future examination (*40*, *41*). One can say about these invariants that they emerge only from a kind of analytic continuation of the bipartite concurrence function $C(t)$ to un-physically negative values, which is permitted via $Q(t)$. The entanglement flow issue (*42*) is also related to, and appears to expand considerably, the theory associated with entanglement swapping, which is under active exploration, and has been realized with particle pairs from independent sources (*43*).

Non-Markovian noises. Dissipative entanglement evolution is critically dependent on the types of the noises acting on the system. Markov environments are those for which a noise signal has no self-correlation over any time interval, and under Markov conditions noise typically results in a quantum irreversible process. Non-Markovian noise arising from a structured environment or from strong coupling appears to be more fundamental (*44*, *45*). Recent studies have suggested that correlated noises may cause new difficulties in using quantum error correction codes (*46*) and dynamic decoupling (*47*). Although some progress has been made, extending the current research on ESD into physically relevant non-Markovian situations remains a challenge. High-Q cavity QED and quantum dot systems are two possible experimental venues.

Qutrits and beyond. Many-qubit entanglement and entanglement of quantum systems that are not qubits (i.e., those having more than two states) is largely an open question, and one that is embarrassing in a sense, because the question has been open since quantum mechanics was invented in the 1920s. There is still no known finite algorithm for answering the simple-seeming question of whether a given mixed state is entangled or not, if it refers to more than two systems, and it is answerable for two mixed-state systems only in the case of pairs of qubits (as we have been discussing) and the case of one qubit and one qutrit (a three-state system such as spin-1). Investigation into ESD of qubit-qutrit systems has begun (*48*, *49*), but generalizations to many-qubit systems are daunting tasks due to both technical and conceptual difficulties (*7*–*9*).

Topological approach. *N*-party entanglement dynamics will presumably become simpler to predict if a computable entanglement measure for a mixed state of more than two qubits can be discovered. However, an alternative approach is to avoid dynamics through topological analysis (*50*). One now knows (*51*, *52*) that ESD is necessary (i.e., must occur) in arbitrary *N*-party systems of noninteracting qubits if they are exposed to thermal noise at any finite $T > 0$ temperature. The steady state of any noninteracting *N*-qubit system has a neighborhood in which every state is separable. In this case, any prearranged subsystem entanglement will inevitably be destroyed in a finite time. This is a universal result showing how entanglement evolves in the absence of external noise control.

Clearly, the holy grail for research on entanglement dynamics is to find an efficient real-time technique for tracking and controlling the entanglement evolution of a generic many-qubit system. Another important open question is to determine a generic method for direct experimental registration of entanglement, for which there is no current answer. We believe that many surprising results are awaiting discovery.

References and Notes

1. E. Schrödinger, *Naturwissenschaften* **23**, 807 (1935).
2. A. Einstein, B. Podolsky, N. Rosen, *Phys. Rev.* **47**, 777 (1935).
3. M. A. Nielsen, I. L. Chuang, *Quantum Computation and Quantum Information* (Cambridge Univ. Press, Cambridge, 2000).
4. C. H. Bennett, D. P. DiVincenzo, *Nature* **404**, 247 (2000).
5. W. H. Zurek, *Rev. Mod. Phys.* **75**, 715 (2003).
6. T. Yu, J. H. Eberly, *Phys. Rev. B* **66**, 193306 (2002).
7. C. Simon, J. Kempe, *Phys. Rev. A* **65**, 052327 (2002).
8. W. Dür, H. J. Briegel, *Phys. Rev. Lett.* **92**, 180403 (2004).
9. For an earlier review of entanglement dynamics, see (*53*).
10. T. Yu, J. H. Eberly, *Phys. Rev. Lett.* **93**, 140404 (2004).
11. K. Zyczkowski, P. Horodecki, M. Horodecki, R. Horodecki, *Phys. Rev. A* **65**, 012101 (2001).
12. A. K. Rajagopal, R. W. Rendell, *Phys. Rev. A* **63**, 022116 (2001).
13. L. Diosi, in *Irreversible Quantum Dynamics*, F. Benatti, R. Floreanini, Eds. (Springer, New York, 2003), pp. 157–163.
14. S. Daffer, K. Wodkiewicz, J. K. McIver, *Phys. Rev. A* **67**, 062312 (2003).
15. P. J. Dodd, J. J. Halliwell, *Phys. Rev. A* **69**, 052105 (2004).
16. T. Yu, J. H. Eberly, *Phys. Rev. Lett.* **97**, 140403 (2006).
17. For details, see section 1 of the Supporting Online Material.
18. M. P. Almeida *et al.*, *Science* **316**, 579 (2007).
19. J. Laurat, K. S. Choi, H. Deng, C. W. Chou, H. J. Kimble, *Phys. Rev. Lett.* **99**, 180504 (2007).
20. J. H. Eberly, T. Yu, *Science* **316**, 555 (2007).
21. Our example illustrates the distinction between entangled and nonentangled states, but quantum entanglement has the ability to encode oppositeness that goes further than the awake-asleep dichotomy of the cats or the heads-tails dichotomy of coins. One extension is the anti-alignment of the hands of a clock, not uniquely found at 6:00, but realized also at different angles of the hands, at approximately 7:05, 8:10, etc. Orthogonal photon polarizations, which may be oriented to any direction, extend the concept to continuous "opposites," exploited by Clauser and Freedman in their famous experiment showing quantum violation of a Bell Inequality (*54*).
22. Matrix encoding of the entanglement is more complicated than the bracket notation used for the cats, but it is important because we want to allow for more possibilities, which can be visualized by thinking that any of the four joint state labels ++, +−, −+, or −− can be correlated with itself or any other, making 16 basic correlation labels, and these are conventionally arranged in a 4 × 4 matrix. This is the density matrix ρ referred to in the text. See the Supporting Online Material for an example, and a sketch of the theory of time evolution of the density matrix in a noisy environment.
23. W. K. Wootters, *Phys. Rev. Lett.* **80**, 2245 (1998).
24. T. Yu, J. H. Eberly, *Opt. Commun.* **264**, 393 (2006).
25. J. Preskill, *Proc. R. Soc. Lond. A* **454**, 385 (1998).
26. I. Sainz, G. Björk, *Phys. Rev. A* **77**, 052307 (2008).
27. D. A. Lidar, K. B. Whaley, in *Irreversible Quantum Dynamics*, F. Benatti, R. Floreanini, Eds. (Springer, Berlin, 2003), pp. 83–120.
28. G. Gordon, G. Kurizki, *Phys. Rev. Lett.* **97**, 110503 (2006).
29. S. Maniscalco, F. Francica, R. L. Zaffino, N. Lo Gullo, F. Plastina, *Phys. Rev. Lett.* **100**, 090503 (2008).
30. For example, see L. Viola, S. Lloyd, *Phys. Rev. A* **58**, 2733 (1998).
31. A. R. R. Carvalho, A. J. S. Reid, J. J. Hope, *Phys. Rev. A* **78**, 012334 (2008).
32. E. T. Jaynes, F. W. Cummings, *Proc. IEEE* **51**, 89 (1963).
33. M. Yönac, T. Yu, J. H. Eberly, *J. Phys. B* **39**, S621 (2006).
34. Z. Ficek, R. Tanas, *Phys. Rev. A* **74**, 024304 (2006).
35. M. Yönac, T. Yu, J. H. Eberly, *J. Phys. B* **40**, S45 (2007).
36. M. Yönac, J. H. Eberly, *Opt. Lett.* **33**, 270 (2008).
37. H. Nha, H. J. Carmichael, *Phys. Rev. Lett.* **93**, 120408 (2004).
38. T. Yu, J. H. Eberly, *Quant. Inf. Comput.* **7**, 459 (2007).
39. A. R. P. Rau, M. Ali, G. Alber, *Eur. J. Phys.* **82**, 40002 (2008).
40. I. Sainz, G. Björk, *Phys. Rev. A* **76**, 042313 (2007).
41. D. Cavalcanti *et al.*, *Phys. Rev. A* **74**, 042328 (2006).
42. T. S. Cubitt, F. Verstraete, J. I. Cirac, *Phys. Rev. A* **71**, 052308 (2005).
43. M. Halder *et al.*, *Nat. Phys.* **3**, 692 (2007).
44. M. Ban, *J. Phys. A* **39**, 1927 (2006).
45. B. Bellomo, R. Lo Franco, G. Compagno, *Phys. Rev. Lett.* **99**, 160502 (2007).
46. E. Novais, E. R. Mucciolo, H. U. Baranger, *Phys. Rev. A* **78**, 012314 (2008).
47. K. Shiokawa, B. L. Hu, *Quant. Inf. Proc.* **6**, 55 (2007).
48. K. Ann, G. Jaeger, *Phys. Rev. B* **75**, 115307 (2007).
49. A. Checinska, K. Wodkiewicz, *Phys. Rev. A* **76**, 052306 (2007).
50. B. V. Fine, F. Mintert, A. Buchleitner, *Phys. Rev. B* **71**, 153105 (2005).
51. T. Yu, J. H. Eberly, http://arxiv.org/abs/0707.3215 (2007).
52. A. Al-Qasimi, D. F. V. James, *Phys. Rev. A* **77**, 012117 (2008).
53. F. Mintert, A. R. R. Carvalho, M. Kus, A. Buchleitner, *Phys. Rep.* **415**, 207 (2005).
54. S. J. Freedman, J. F. Clauser, *Phys. Rev. Lett.* **28**, 938 (1972).

55. T.Y. and J.H.E. acknowledge grant support from the U.S. Army Research Office (48422-PH), the NSF (PHY06-01804 and PHY07-58016), and U.S. Department of Energy, Office of Basic Energy Sciences (DE-FG02-05ER15713).

Supporting Online Material

www.sciencemag.org/cgi/content/full/323/5914/598/DC1
SOM Text
Fig. S1
References

10.1126/science.1167343

Evolution of Long-Time Non-Interacting Quantum Entanglement

Muhammed Yönaç and J.H. Eberly
Rochester Theory Center, and Department of Physics and Astronomy,
University of Rochester, New York 14627, USA

We report calculations of the long-time evolution of quantum entanglement. We employ a simple model that permits partially analytic examination of entanglement transfer among a combination of discrete-state and continuous-state non-localized degrees of freedom of a four-part quantum system. Among the results are the development of a novel approximation scheme, the re-appearance of entanglement after lengthy intervals of zero entanglement, and formulas for relatively slow loss of entanglement and duration of revival intervals.

PACS numbers: 42.50.Ex, 42.50.Pq, 03.65.Ud, 42.50.Ct.

I. INTRODUCTION

Almost 75 years after its description by Schrödinger [1] there is still no general understanding of entanglement within quantum theory in the sense that measures of it are still being developed. Only two-particle entanglement is well quantified, and even in that case the number of states that can be taken into account is extremely small unless the joint state is pure. The behavior of few-state entangled quantum systems takes a wide variety of forms in different environments, and it is well known that some of them are being studied to achieve advances in computing and communications. Whether such goals are of interest or not, the controlled manipulation of entanglement with external agents is one approach to an ultimate form of quantum control, and it remains a fascinating challenge.

We will examine aspects of what we can call pure storage of quantum information, a context that might have relevance in computing and communication. More generally this means that we are interested in evolution of two-party entanglement of simple examples of quantum systems such as two-level atoms and coherent states of radiation, but in this case under the conditions of mutual isolation and non-interaction between the joint information storing systems. The term qubit serves as a useful general term for two-level quantum systems whether in atoms, molecules, impurity sites in crystals, quantum dots, SQUIDs, photon polarizations or of course spins, so we will adopt it for a discussion of long-time two-qubit evolution under the no-interaction stipulation.

Earlier discussions usually allowed or relied on mutual interactions to produce entanglement dynamics or control it. Kim, et al., showed [2] that an incoherent thermal field can create entanglement between two such qubits. Entanglement transfer between two qubits and two separate fields was examined by Zhou and Wang [3]. In their treatment the quantum field was weak rather than strong. The evolution of entanglement in a qubit-field system, where the qubit and the field start from mixed states was examined by Rendell and Rajagopal [4]. They aimed to calculate the entanglement embedded in the full system, and because of the lack of an entanglement measure for $2 \times \infty$ systems they calculated a lower bound for the concurrence instead. The controlled manipulation of entanglement with external agents is a common goal of most of these studies.

We first review entanglement dynamics in an idealized situation in order to establish notation for control parameters, time scales, etc. Thus, each site of our network contains a qubit in the physical form of a two-level atom (ion qubit, spin qubit and photonic qubit analogs are easily imagined). We restrict attention to the dynamics of entanglement between two of the sites, say A and B. We suppose that there is quantum memory present in the qubits that is of interest, i.e., that the two atoms have been entangled in some way before being inserted into their respective cavities. Field modes a and b are available at the A-B sites that can be used for interacting with the atoms (i.e., for "controlling" them and their entanglement externally). This scenario is suggested in Fig. 1.

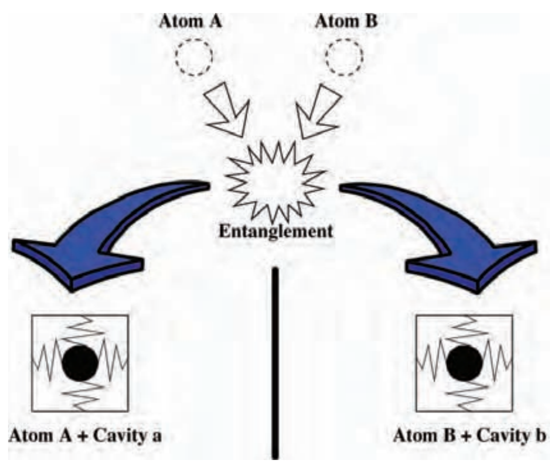

FIG. 1: A diagram illustrating our system. The atoms A and B are placed in their respective cavities a and b after being entangled. Only A-a and B-b interactions take place thereafter, causing non-interacting A-B entanglement to change in time.

II. HAMILTONIAN EQUATIONS

The Jaynes-Cummings [5] interaction governs evolution in our system. The Hamiltonian (with $\hbar = 1$) is given by:

$$\begin{aligned} H_{\rm tot} &= \frac{\omega_0}{2}\sigma_z^A + g(a^\dagger\sigma_-^A + \sigma_+^A a) + \omega a^\dagger a \\ &+\frac{\omega_0}{2}\sigma_z^B + g(b^\dagger\sigma_-^B + \sigma_+^B b) + \omega b^\dagger b, \end{aligned} \quad (1)$$

where ω_0 is the transition frequency between the two levels of the atoms, g is the constant of coupling between the atoms and the fields and ω is the angular frequency of the single-mode field. The usual Pauli matrices $\sigma_z^{A,B}$, $\sigma_+^{A,B}$ and $\sigma_-^{A,B}$ describe the atoms, while $a^\dagger$, a and $b^\dagger$, b are the raising and lowering operators for the fields.

Note that the Hamiltonian does not support any interaction between atom A and atom B or between mode a and mode b. Physical realization of our scenario does not appear out of the question, as the Jaynes-Cummings model has been realized in the laboratory in several well-known ways [6–9].

To illustrate the approach to be followed when the fields are taken as coherent states, we start with a simpler example, in which the field modes are initially in their vacuum states: $|0_a\rangle \otimes |0_b\rangle$, and the two atoms are in a superposition of Bell states. For the vacuum case the coupling terms in our Hamiltonian indicate that for creation of a photon in a cavity the atom in that cavity must decay to a lower state. Since the cavities each contain only one atom, there can be no more than one photon in each at any time. This means that the cavities are also two-state quantum systems, i.e., qubits.

The eigenstates of the JC Hamiltonian are well known. We will write for either Aa or Bb

$$H_{\rm JC}|\psi_n^\pm\rangle = \lambda_n^\pm|\psi_n^\pm\rangle. \quad (2)$$

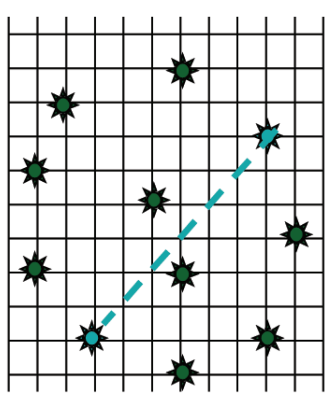

FIG. 2: Sketch indicating non-interacting qubits in a quantum storage network. Quantum memory in the form of two-qubit entanglement between any two relatively remote sites, indicated here by a dashed line, can be altered by fields local to the sites.

We will denote the excited and ground atomic states by $|e\rangle$ and $|g\rangle$, and denote the cavity modes' photon states by the photon number n. Then the JC eigenvalues are given by:

$$\lambda_n^\pm = n\omega + \frac{1}{2}\Big(\Delta \pm \sqrt{\Delta^2 + G_n^2}\Big), \quad (3)$$

where $\Delta = \omega_0 - \omega$ is the detuning and

$$G_n = 2g\sqrt{n}, \quad (4)$$

is the n-photon Rabi frequency.

The JC eigenstates have the following form as superpositions of the bare atom and cavity states:

$$\begin{aligned} |\psi_0\rangle &= |g;0\rangle & (5)\\ |\psi_n^+\rangle &= c_n|e;n-1\rangle + s_n|g;n\rangle \ \ (n>0) & (6)\\ |\psi_n^-\rangle &= -s_n|e;n-1\rangle + |c_n|g;n\rangle \ \ (n>0). & (7) \end{aligned}$$

In these equations we have introduced some convenient abbreviations:

$$c_n \equiv \cos(\theta_n/2) \quad \text{and} \quad s_n \equiv \sin(\theta_n/2), \quad (8)$$

where the rotation angle θ_n can be identified with the Bloch sphere polar angle and is defined in the usual way:

$$\cos\theta_n \equiv \frac{\Delta}{\sqrt{\Delta^2 + G_n^2}} \quad \text{and} \quad \sin\theta_n \equiv \frac{G_n}{\sqrt{\Delta^2 + G_n^2}}. \quad (9)$$

In this preliminary example we will need the true ground state $|\psi_0\rangle = |g;0\rangle$ and the two dressed states for $n = 1$. These three states are closed under the JC Hamiltonian for each site. In other words, we use only $n = 1$ in the equations above, so the subscript n can mostly be ignored and we will frequently drop it ($\lambda_n \to \lambda$, $c_n \to c$, etc.).

III. MEASURE OF PAIRWISE ENTANGLEMENT

The JC dressed states are atom-photon locally-entangled states themselves, and this entanglement has interesting consequences if the cavities are fairly highly excited, as Gea-Banacloche [10] and Phoenix and Knight [11] originally pointed out. Here we are interested in non-local atom-atom entanglement between the two spatially separated sites on a qubit lattice, as suggested in Fig. 2.

In the general context of entanglement we note that there is no accepted and practically workable criterion for determining separability of arbitrary four-particle states. Our purposes will be satisfied by working with the two-qubit atomic states obtained from the time-evolving four-qubit state. All familiar measures agree about separability in the two-qubit domain of entanglement. That is, entropy of formation, Schmidt number, tangle, negativity, and concurrence are numerically somewhat different, but in the two-qubit domains of their applicability they are in full agreement when they signal complete separability, i.e., the lack of entanglement.

We adopt Wootters' concurrence [12] as our measure in this discussion, mainly for its convenient normalization: $1 \geq C \geq 0$, where $C = 0$ indicates separability (zero entanglement) and $C = 1$ means maximal pure state entanglement, as in a Bell state; and simplicity of calculation:

$$C(\rho) = \max\{0, \sqrt{\lambda_1} - \sqrt{\lambda_2} - \sqrt{\lambda_3} - \sqrt{\lambda_4}\}, \qquad (10)$$

where the quantities λ_i are the eigenvalues in decreasing order of the auxilliary matrix

$$\zeta = \rho(\sigma_y \otimes \sigma_y)\rho^*(\sigma_y \otimes \sigma_y), \qquad (11)$$

where ρ^* denotes the complex conjugation of ρ in the standard basis and σ_y is the Pauli matrix expressed in the standard basis.

One finds that in reduction to two-qubit form, by tracing over the two field-mode qubits, the resulting two-qubit mixed state always has the X form [13], where only the diagonal and anti-diagonal elements are not zero:

$$\rho = \begin{bmatrix} a & 0 & 0 & w \\ 0 & b & z & 0 \\ 0 & z^* & c & 0 \\ w^* & 0 & 0 & d \end{bmatrix}, \qquad (12)$$

where $a + b + c + d = 1$. The concurrence of this mixed state is easily found to be

$$C = 2\max\{0, |z| - \sqrt{ad}, |w| - \sqrt{bc}\} \equiv 2\max\{0, Q\}, \quad (13)$$

so it is clear that Q, which is the larger of $|z| - \sqrt{ad}$ and $|w| - \sqrt{bc}$, will be an important quantity. For example, $Q(t)$ obeys certain conservation relations (whereas C does not) in some special cases because it can be negative. Furthermore, one can see [14] that while $Q \leq 0$ implies a separable state ($C = 0$), the slightly stronger condition $Q < 0$ implies both $C = 0$ and also that the state is mixed rather than pure, information not available from C.

In the two-site situation under consideration there are, in principle, six different concurrences that can provide information about the bipartite entanglements that may arise. With an obvious notation we can denote these as C^{AB}, C^{ab}, C^{Aa}, C^{Bb}, C^{Ab}, C^{Ba}. Except for C^{Aa} and C^{Bb}, they measure remote (non-local) entanglements.

IV. PARTIALLY ENTANGLED BELL STATES

Aspects of the entanglement dynamics of qubits in the vacuum two-cavity case have been reported already [15–17]. For background we summarize results when the initial states are superpositions of the Bell states: $|\Phi^{\pm}\rangle \sim |e_A, e_B\rangle \pm |g_A, g_B\rangle$, which we write:

$$|\Phi_{AB}\rangle = \cos\alpha|e_A, e_B\rangle + \sin\alpha|g_A, g_B\rangle. \qquad (14)$$

It is easy to see that $\alpha = \pm\pi/4$ reproduces the two pure Bell states.

The initial state for the atoms plus cavities is therefore:

$$\begin{aligned} |\Phi(0)\rangle &= |\Phi_{AB}\rangle \otimes |0_a, 0_b\rangle \\ &= (\cos\alpha|e_A, e_B\rangle + \sin\alpha|g_A, g_B\rangle) \otimes |0_a, 0_b\rangle. \end{aligned} \qquad (15)$$

In terms of the dressed eigenstates given above (5), we can rewrite:

$$\begin{aligned} |e_A, 0_a\rangle &= c|\psi_1^+\rangle - s|\psi_1^-\rangle \\ |g_A, 1_a\rangle &= s|\psi_1^+\rangle + c|\psi_1^-\rangle \quad \text{and} \\ |g_A, 0_a\rangle &= |\psi_0\rangle. \end{aligned} \qquad (16)$$

Thus the initial atom-atom entangled state has the form

$$\begin{aligned} &\cos\alpha|e_A, 0_a\rangle \otimes |e_B, 0_b\rangle + \sin\alpha|g_A, 0_a\rangle \otimes |g_B, 0_b\rangle \\ &= \cos\alpha(c|\psi_1^+\rangle_A - s|\psi_1^-\rangle_A) \otimes (c|\psi_1^+\rangle_B - s|\psi_1^-\rangle_B) \\ &\quad + \sin\alpha|\psi^0\rangle_A \otimes |\psi^0\rangle_B. \end{aligned} \qquad (17)$$

Evolution in time is easily followed through the evolution of the dressed states:

$$|\psi^{\pm}(t)\rangle = e^{-i\lambda^{\pm}t}\, |\psi^{\pm}(0)\rangle. \qquad (18)$$

Note that since the combination of coefficients in $|\Phi(0)\rangle$ uniquely associates c with $|\psi^+\rangle$, and s with $|\psi^-\rangle$, the time evolution can be transferred to the c and s symbols. We will henceforth consider them carrying the time-evolution exponents. We will use the notation $c_0 \equiv c(0)$ and $s_0 \equiv s(0)$ to refer to their values at $t = 0$ (no relation to the $n = 0$ subscripts in Eq. (8)), so that,

$$\begin{aligned} c = c(t) &= c_0 e^{-i\lambda^+ t}, \\ s = s(t) &= s_0 e^{-i\lambda^- t}, \end{aligned} \qquad (19)$$

where λ^+ and λ^- are obtained by inserting $n = 1$ into Eq. (3). Then we can write (temporarily again indicating explicit time dependences for the c's and s's):

$$\begin{aligned} |\Phi(t)\rangle &= \cos\alpha\Big(c(t)|\psi_1^+\rangle_A - s(t)|\psi_1^-\rangle_A\Big) \\ &\otimes \Big(c(t)|\psi_1^+\rangle_B - s(t)|\psi_1^-\rangle_B\Big) \\ &+ \sin\alpha|\psi^0\rangle_A \otimes |\psi^0\rangle_B, \end{aligned} \qquad (20)$$

where $|\psi^{\pm}\rangle$ will continue to refer to the JC states at $t = 0$.

Now we revert to the bare basis states in preparation for the tracing needed to calculate Q^{AB} and C^{AB}:

$$\begin{aligned} |\Phi(t)\rangle &= \cos\alpha\Big(c(t)(c_0|e_A, 0_a\rangle + s_0|g_A, 1_a\rangle) \\ &- s(t)(-s_0|e_A, 0_a + c_0|g_A, 1_a\rangle)\Big) \otimes \Big(c(t)(c_0|e_B, 0_b\rangle \\ &+ s_0|g_B, 1_b\rangle) - s(t)(-s_0|e_B, 0_b + c_0|g_B, 1_b\rangle)\Big) \\ &+ \sin\alpha|g_A, 0_a\rangle \otimes |g_B, 0_b\rangle \\ &= \cos\alpha\Big((cc_0 + ss_0)|e_A, 0_a\rangle + (cs_0 - sc_0)|g_A, 1_a\rangle\Big) \\ &\otimes \Big((cc_0 + ss_0)|e_B, 0_b\rangle + (cs_0 - sc_0)|g_B, 1_b\rangle\Big) \\ &+ \sin\alpha|g_A, 0_a\rangle \otimes |g_B, 0_b\rangle. \end{aligned} \qquad (21)$$

To get the two-qubit mixed state needed for calculation of Q^{AB} the projections that are needed are:

$$\begin{aligned}
\langle 0_a, 0_b|\Phi(t)\rangle &= \cos\alpha(cc_0 + ss_0)^2|e_a, e_B\rangle + \sin\alpha|g_A, g_B\rangle \\
\langle 1_a, 0_b|\Phi(t)\rangle &= \cos\alpha(cs_0 - sc_0)(cc_0 + ss_0)|g_A, e_B\rangle \\
\langle 0_a, 1_b|\Phi(t)\rangle &= \cos\alpha(cc_0 + ss_0)(cs_0 - sc_0)|e_A, g_B\rangle \\
\langle 1_a, 1_b|\Phi(t)\rangle &= 0. \qquad (22)
\end{aligned}$$

These show that the AB mixed state has the X form mentioned in the previous Section:

$$\rho^{AB} = \begin{bmatrix} a & 0 & 0 & w \\ 0 & b & 0 & 0 \\ 0 & 0 & c & 0 \\ w^* & 0 & 0 & d \end{bmatrix}, \qquad (23)$$

for which the concurrence has the stated form

$$C^{AB} = 2\ max\{0, |w| - \sqrt{bc}\}. \qquad (24)$$

and we easily find the following

$$\begin{aligned}
|w| &= |\sin\alpha\cos\alpha|(c_0^4 + s_0^4 + 2c_0^2 s_0^2 \cos\delta t), \\
b = c &= \cos^2\alpha|cc_0 + ss_0|^2\ |cs_0 - sc_0|^2 \\
&= \cos^2\alpha(c_0^4 + s_0^4 + 2c_0^2 s_0^2\cos\delta t) \\
&\times\ c_0^2 s_0^2(2 - 2\cos\delta t), \qquad (25)
\end{aligned}$$

where $\delta = \sqrt{\Delta^2 + 4g^2}$.

For simplicity we will evaluate this in the resonance case, $\theta_n = \pi/2$, where $c_0 = s_0 = 1/\sqrt{2}$ and $\Delta = 0$. Then we find

$$|w| - \sqrt{bc} = \frac{1}{4}\cos^2\alpha[2 + 2\cos(gt)][|\tan\alpha| - \sin^2(gt)], \qquad (26)$$

from which the expression for concurrence is found to be:

$$C^{AB} = 2\max\{0, Q^{AB}\}, \qquad (27)$$

where $Q^{AB} = \cos^2\alpha\cos^2(gt)[|\tan\alpha| - \sin^2(gt)]$.

Fig. 3 shows that for $\alpha \neq \pi/4$ the C^{AB} curves have the "sudden death" feature [18]. That is, the entanglement non-smoothly becomes zero and stays zero for a finite interval of time. It is also clear that the AB and ab entanglements are opposites in the sense that one increases as the other decreases (except in the regions where both are zero). This has been analyzed in terms of information transport, and time-invariant relations have been identified [15] that connect all six $Q(t)$ values. Because the evolution in the ideal situation treated here is lossless, and only finitely many states are involved, the periodic nature of the curves is not surprising. However, the situation is more realistic when infinitely many final states are involved (quantum open system case). Results are available in cases involving simple harmonic oscillators that interact with reservoirs [19, 20]. In the remaining sections we will employ the techniques presented here to extend the vacuum results into the open-system domain by allowing the atoms to interact with (be controlled by) more realistic fields, namely fields described by quantum coherent states.

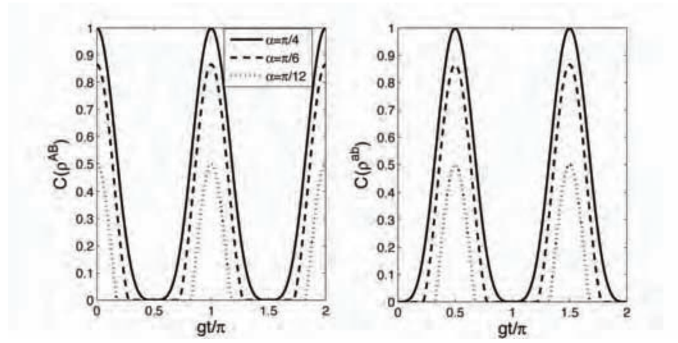

FIG. 3: Time dependences of AB and ab concurrences for three values of the superposition angle α. Note that almost all curves have some time interval over which C=0, i.e., during which the underlying state must be separable. From ref. [15].

V. OPEN-SYSTEM TWO-QUBIT THEORY

Realistic quantum control almost necessarily implies engagement of continuous variables and the interaction of qubits or other systems having a finite number of states with one or more "large" systems with continuous quantum states. Novel bipartite aspects of open-system joint qubit states have been noted recently [21]. We can use the JC formalism described above to enter this domain by introducing coherent state fields at the AB network sites. The Jaynes-Cummings interaction remains relevant, and we again focus on pure storage memory nets, with sites entangled but not interacting, as in Fig. 2.

We retain almost all of the simplifying approximations made earlier, and add one more by taking the two fields, now modeled as coherent state fields, to have the same average photon number $\bar{n}$. However, one important simplification that we relied on previously must now be discarded. The coherent-state fields have many occupied photon-number states, so the cavities will not be qubits. We assume initial atom entanglement in the form of a pure Bell State:

$$|\Psi_{AB}(0)\rangle = (|eg\rangle + |ge\rangle)/\sqrt{2}, \qquad (28)$$

and write the field state as the coherent state product

$$|\Psi_{ab}(0)\rangle = |\alpha\rangle \otimes |\alpha\rangle. \qquad (29)$$

As a result our initial state for the whole system is,

$$|\Psi_{tot}(0)\rangle = |\Psi_{AB}(0)\rangle \otimes |\alpha\rangle \otimes |\alpha\rangle. \qquad (30)$$

The coherent states are given by the familiar Fock state expansion

$$|\alpha\rangle = \sum_{n=0}^{\infty} A_n|n\rangle = \sum_{n=0}^{\infty}\frac{e^{-|\alpha|^2/2}\alpha^n}{\sqrt{n!}}|n\rangle. \qquad (31)$$

Because a coherent state provides an infinite number of Fock states, the photonic density matrix becomes infinite-dimensional, and the joint AB dynamics extremely complicated. Fully numerical analysis is possible, but the insights from analytic results are highly desirable. We have found a key step permitting analytic progress. This is an apparently drastic simplification of the continuous state spaces of the two field modes. We assume that it is satisfactory to replace $|\alpha\rangle$ by $|\bar{n}\rangle$. This Ansatz is at least weakly supported by the knowledge that photon number in a coherent state is Poisson-distributed and relatively tightly centered around $\bar{n}$ when $\bar{n} \gg 1$. Thus we represent the initial field state by the single product Fock state $|\bar{n}\rangle \otimes |\bar{n}\rangle$. Note that during the JC interaction the photon number in either field mode a or b can then be $\bar{n}$ or $\bar{n}+1$ or $\bar{n}-1$. Thus the field modes are no longer convenient qubits as they were in Sec. IV.

Under the Ansatz mentioned, by tracing the field mode states, we find that the reduced density matrix for the qubits becomes:

$$\rho = \begin{pmatrix} a & x & x & x \\ x & b & z & x \\ x & z* & c & x \\ x & x & x & d \end{pmatrix} \rightarrow \begin{pmatrix} a & 0 & 0 & 0 \\ 0 & b & z & 0 \\ 0 & z* & c & 0 \\ 0 & 0 & 0 & d \end{pmatrix}, \qquad (32)$$

where we have used the standard two-qubit basis $[ee,\ eg,\ ge,\ gg]$. The elements indicated by x are zero because of the equal-$\bar{n}$ simplification. Thus, under the assumptions mentioned, ρ is again of X-type [13]).

For this X-type ρ, concurrence turns into:

$$C(\rho) = 2\ max[\ 0,\ |z| - \sqrt{ad}\ ]. \qquad (33)$$

The coherent fields induce time-dependent change of the elements a and d, and their growth and any decline of z will cause entanglement to decrease.

In order to calculate the time evolution of this state under the JC Hamiltonian we need to calculate the time evolution of the the states of the individual sites, i.e., $|e\rangle \otimes |n\rangle$ and $|g\rangle \otimes |n\rangle$ for all n. The time evolution of these states for site A (and similarly for site B) is given by,

$$\begin{aligned} e^{iH_I^A t}|e;n\rangle &= \cos(gt\sqrt{n+1})|e;n\rangle \\ &- i\sin(gt\sqrt{n+1})|g;n+1\rangle \qquad (34) \\ e^{iH_I^A t}|g;n\rangle &= \cos(gt\sqrt{n})|g;n\rangle \\ &- i\sin(gt\sqrt{n})|e;n-1\rangle. \qquad (35) \end{aligned}$$

Using these results, the time evolution of the initial state of the system is found to be,

$$\begin{aligned} |\Psi_{tot}(t)\rangle &= e^{iH_I^A t}|\Psi_{tot}(0)\rangle \qquad (36) \\ &= \frac{1}{\sqrt{2}}\sum_{n=0}^{\infty}\sum_{m=0}^{\infty} A_n A_m \Big(K_{mn}\Big), \qquad (37) \end{aligned}$$

where

$$\begin{aligned} K_{mn} &= -iC_{n+1}S_m|e,e;n,m-1\rangle + C_{n+1}S_m|e,g;n,m\rangle \\ &- S_{n+1}S_n|g,e;n+1,m\rangle - iS_{n+1}C_n|g,g;n+1,m\rangle \\ &- iS_nC_{m+1}|e,e;n-1,m+1\rangle \\ &- S_nS_{m+1}|e,g;n-1,m+1\rangle \\ &+ C_nC_{m+1}|g,e;n,m+1\rangle \\ &- iC_nS_{m+1}|g,g;n,m+1\rangle, \qquad (38) \end{aligned}$$

where $C_n = \cos(gt\sqrt{n})$ and $S_n = \sin(gt\sqrt{n})$. The density matrix for the system is then given by

$$\rho_{tot} = |\Psi_{tot}(t)\rangle\langle|\Psi_{tot}(t)|. \qquad (39)$$

and the reduced density matrix for the atoms, ρ_{AB}, is given by,

$$\rho_{AB} = Tr_{(n,m)}\rho_{tot}. \qquad (40)$$

Having used the Fock state shortcut to obtain (32), we avoid using it further now and calculate the elements $z,\ a,\ d$ of ρ_{AB} for the coherent state. The z term is given by the doubly infinite summation,

$$\begin{aligned} z &= \frac{1}{2}\Big\{\sum_{n,m} A_n^2A_m^2C_nC_{n+1}C_mC_{m+1} \\ &- A_nA_{n-1}A_mA_{m+1}S_nC_{n+1}C_mS_{m+1} \\ &+ A_nA_{n-2}A_mA_{m+2}S_nS_{n-1}S_{m+1}S_{m+2} \\ &- A_nA_{n-1}A_mA_{m+1}S_nC_{n-1}S_{m+1}C_{m+2}\Big\}, \qquad (41) \end{aligned}$$

Similarly the series summations for a and d are:

$$\begin{aligned} a &= \frac{1}{2}\Big\{\sum_{n,m} A_n^2A_m^2C_{n+1}^2S_m^2 \\ &+ A_nA_{n+1}A_mA_{m-1}S_{n+1}C_{n+1}S_mC_m \\ &+ A_n^2A_m^2S_n^2C_{m+1}^2 \\ &+ A_nA_{n-1}A_mA_{m+1}S_nC_nS_{m+1}C_{m+1}\Big\} \qquad (42) \end{aligned}$$

and

$$\begin{aligned} d &= \frac{1}{2}\Big\{\sum_{n,m} A_n^2A_m^2S_{n+1}^2C_m^2 \\ &+ A_nA_{n+1}A_mA_{m-1}S_{n+1}C_{n+1}S_mC_m \\ &+ A_n^2A_m^2C_n^2S_{m+1}^2 \\ &+ A_nA_{n-1}A_mA_{m+1}S_nC_nS_{m+1}C_{m+1}\Big\}. \qquad (43) \end{aligned}$$

The infinite extent of these summations of course reflects the fact that we are dealing with a quantum open system, by having coupled the qubits to an infinite state space.

The sums above cannot be completed, but excellent analytic approximations can be found for coherent states that are even only moderately strong, i.e., $\alpha \geq 10$. We will use the familiar Stirling formula for $n!$,

$$n! = \sqrt{2\pi n}n^ne^{-n}, \qquad (44)$$

and Euler's formula to approximate the terms in the summations above by integrals. We begin by approximating the terms like $A_nA_{n+1}A_mA_{m-1}$ with $A_n^2A_m^2$, which introduces an error of order $1/\bar{n}$ near the Poisson peaks $n \approx m \approx \bar{n}$. Then we get for z

$$\begin{aligned} z \;&\cong\; \frac{1}{2}\Big\{\Big(\sum_n A_n^2 C_n C_{n+1}\Big)^2 \\ &-\; 2\Big(\sum_{n,m} A_n^2 A_m^2 S_n C_{n+1} C_m S_{m+1}\Big) \\ &+\; \Big(\sum_n A_n^2 S_n S_{n+1}\Big)^2\Big\}. \end{aligned} \tag{45}$$

In the same way, Eq.(42) and Eq.(43) become,

$$a \cong \Big((\sum_n A_n C_n^2\Big)\Big(\sum_n A_n^2 S_n^2\Big) + \Big(\sum_n A_n^2 S_n C_n\Big)^2, \tag{46}$$

$$d \cong \Big(\sum_n A_n C_n^2\Big)\Big(\sum_n A_n^2 S_n^2\Big) + \Big(\sum_n A_n^2 S_n C_n\Big)^2. \tag{47}$$

Note that Eq. (46) and Eq. (47) imply that $a \cong d$ whenever our large $\bar{n}$ approximation is valid. Now we rewrite C_nC_{n+1} as,

$$\begin{aligned} C_nC_{n+1} \;&=\; \frac{1}{2}\Big\{\cos[gt(\sqrt{n}+\sqrt{n+1})] \\ &+\; \cos[gt(\sqrt{n+1}-\sqrt{n})]\Big\}, \end{aligned} \tag{48}$$

and use the peaked nature of A_n to focus on those terms near to $\bar{n}$ to introduce the approximation

$$\sqrt{n+1} = \sqrt{n} + \frac{1}{2\sqrt{n}}, \tag{49}$$

which compresses C_nC_{n+1} to

$$C_nC_{n+1} \cong \frac{1}{2}\Big[\cos(2gt\sqrt{n}) + \cos\Big(\frac{gt}{2\sqrt{n}}\Big)\Big]. \tag{50}$$

Similarly,

$$\begin{aligned} S_nS_{n+1} \;&\cong\; \frac{1}{2}\Big[\cos\Big(\frac{gt}{2\sqrt{n}}\Big) - \cos(2gt\sqrt{n})\Big] \\ S_nC_{n+1} \;&\cong\; \frac{1}{2}\Big[\sin(2gt\sqrt{n}) - \sin\Big(\frac{gt}{2\sqrt{n}}\Big)\Big] \\ S_{n+1}C_n \;&\cong\; \frac{1}{2}\Big[\sin(2gt\sqrt{n}) + \sin\Big(\frac{gt}{2\sqrt{n}}\Big)\Big]. \end{aligned} \tag{51}$$

With these results we can simplify z further:

$$\begin{aligned} z \;&\cong\; \frac{1}{4}\Big[\Big(\sum_n A_n^2\cos(\frac{gt}{2\sqrt{n}})\Big)^2 + \Big(\sum_n A_n^2\sin(\frac{gt}{2\sqrt{n}})\Big)^2 \\ &+\Big(\sum_n A_n^2\cos(2gt\sqrt{n})\Big)^2 \\ &-\Big(\sum_n A_n^2\sin(2gt\sqrt{n})\Big)^2\Big]. \end{aligned} \tag{52}$$

Now, using the identities,

$$\begin{aligned} C_n^2 \;&=\; \frac{1+\cos(2gt\sqrt{n})}{2} \\ S_n^2 \;&=\; \frac{1-\cos(2gt\sqrt{n})}{2}, \end{aligned} \tag{53}$$

we can rewrite a and d as,

$$\begin{aligned} a \;&\cong\; d \cong \frac{1}{4}\Big[1 - \Big(\sum_n A_n^2\cos(2gt\sqrt{n})\Big)^2 \\ &+\Big(\sum_n A_n^2\sin(2gt\sqrt{n})\Big)^2\Big]. \end{aligned} \tag{54}$$

Then Eqs. (52) and (54) lead to:

$$\begin{aligned} z - \sqrt{ad} \;&\cong\; \frac{1}{4}\Big[\Big(\sum_n A_n^2\cos(\frac{gt}{2\sqrt{n}})\Big)^2 \\ &+\Big(\sum_n A_n^2\sin(\frac{gt}{2\sqrt{n}})\Big)^2 \\ &+2\Big(\sum_n A_n^2\cos(2gt\sqrt{n})\Big)^2 \\ &-2\Big(\sum_n A_n^2\sin(2gt\sqrt{n})\Big)^2 - 1\Big]. \end{aligned} \tag{55}$$

We can calculate the sums involved here by rewriting them as integrals, treating the integer n as continuous, again relying on the large value of $\bar{n}$. The first two integrals we need to calculate are,

$$I_1 = \int_0^\infty A_n^2\cos(\frac{gt}{2\sqrt{n}})dn, \quad \text{and} \tag{56}$$

$$I_2 = \int_0^\infty A_n^2\sin(\frac{gt}{2\sqrt{n}})dn. \tag{57}$$

We will combine these integrals, $I_1 + iI_2 \equiv I_{12}$ in order to work with the exponential of $igt/2\sqrt{n}$. This, together with Stirling's approximation on A_n^2, and the abbreviation $\tau \equiv gt$, leads to

$$I_{12} \cong \int_0^\infty e^{-\alpha^2}\frac{\alpha^{2n}}{\sqrt{2\pi n}}\frac{e^n}{n^n}e^{i\tau/2\sqrt{n}}dn. \tag{58}$$

The saddle point method is appropriate to calculate this integral, and some details are reserved for the Appendix. The expression for $I_1 + iI_2$ is found to be,

$$I_{12} \cong \exp\Big(-\frac{\tau^2}{32\alpha^4}\Big)e^{i\tau/2\alpha}. \tag{59}$$

Then helpful cancellations can be identified, and we obtain an approximate expression for $|z| - \sqrt{ad}$:

$$\begin{aligned} |z| - \sqrt{ad} \;&\cong\; \frac{1}{4}\Big[e^{-g^2t^2/16\bar{n}^2} - 1\Big] \\ &+\; \frac{1}{2}\Big[\sum_n A_n^2\cos(2gt\sqrt{n})\Big]^2 \\ &-\; \frac{1}{2}\Big[\sum_n A_n^2\sin(2gt\sqrt{n})\Big]^2. \end{aligned} \tag{60}$$

The summations in (60) involving $\cos(2gt\sqrt{n})$ and $\sin(2gt\sqrt{n})$ can be combined into a single exponent containing the argument $2igt\sqrt{n}$, which is similar to that in (58), but the resulting saddle point analysis is more complicated because now $\sqrt{n}$ is in the numerator. Details are relegated to the Appendix, with the working result:

$$\begin{aligned} z - \sqrt{ad} &\cong \frac{1}{4}\Big\{ \exp\Big(-\frac{\tau^2}{16\alpha^4}\Big) \\ &-1 + e^{-\tau^2/2}\cos(4\alpha\tau)\Big\} \\ &+ \sum_{k=1,2,\dots} \frac{1}{2\pi k}\Big[\exp\Big(-\frac{2(\tau - 2\pi k\alpha)^2}{1+\pi^2 k^2}\Big) \\ &\quad \times \cos[4\alpha(\tau - 2\pi k\alpha)]\Big]. \end{aligned} \tag{61}$$

In writing this last equation we have used the fact that around $\tau = 2\pi k\alpha$ only the term with the corresponding k gives a significant contribution to the sums. The contribution to $\tau = 2\pi k\alpha$ from any other k' is proportional to $\exp\Big(-4\pi^2\alpha^2(k-k')^2/[1+\pi^2(k')^2]\Big)$, so it decays exponentially with the distance from k.

VI. OVERVIEW AND IMPLICATIONS

We have demonstrated the utility of a novel short-cut approach to determine the open-system evolution of entanglement under coherent-state interaction with two remote qubits. The X-state simplification and Fock-state Ansatz we introduced work together in a surprisingly accurate way. Some details of the calculations themselves have been included for inspection, and we can summarize them by greatly over-simplifying the multiple stages involved as follows. The evaluation of concurrence for $\bar{n} \gg 1$ here is generically the same as that presented for zero detuning qubit inversion in the original discussion of quantum revivals [23], so one should be prepared to find revival behavior here, and strong revivals of entanglement are apparent in Fig. 4 below. They show both the predictions of the analytic expressions given above, and also the results of a numeric check on the Fock state Ansatz adopted to initiate the analytic calculations. That is, Fig. 4 shows our analytical results for the function $2(|z| - \sqrt{ad})$ in comparison with the complete numerical evaluation of concurrence without making the X-type approximation. The agreement is not perfect, but the discrepancies are illuminating.

In particular, the results for entanglement contain details not present in well-known results for inversion, and these details appear to work favorably for application to quantum memory management, as to both storage and recovery. This is not difficult to see, as we now indicate.

There is an important scale issue to note in these figures. Both curves in Fig. 4 show long periods of ESD interrupted by intervals of coherent response, i.e., recovery of entanglement. While it is not perfect recovery it is

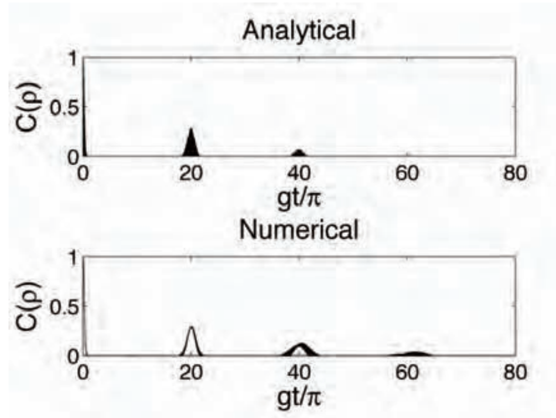

FIG. 4: The analytical and numerical results for concurrence of two qubits exposed to two quantum-coherent driving fields with $\alpha = 10$. The evident revivals are predicted reasonably well by the approximate formula (61). Analytical results are for the X-type ρ while the numerical ones are for the original ρ.

surprisingly robust. The envelope of the revivals decays relatively slowly, as given by the formula

$$\frac{1}{\pi k} - \frac{1 - \exp(-\tau^2/16\alpha^4)}{2}. \tag{62}$$

where k is the revival number.

Returns of concurrence to zero (ESD events) within the analytic revivals are not present in the numeric revivals. The extent of this is seen by inspecting a revival envelope in detail, as is done in Fig. 5. Close to the revival regions the analytical results show rapid oscillations with period $\tau = \pi/(2g\sqrt{n})$ which is half the corresponding period in the inversion case. The analytic formula retains the entanglement death and rebirth episodes that occur on the rapid Rabi-period scale, as were shown in Fig. 3 and have been discussed in the literature repeatedly for few-photon excitation. By contrast, the numeric results show a smoothed version without rapidly recurring ESD events. Even the zero revival, i.e., the period that is referred to as the Cummings collapse in the inversion literature, shows no ESD events within it.

One can conclude that, in principle at least, several aspects of quantum memory management can be further developed for remote qubit entanglement using the interactions employed here. For example, we see that quantum joint memory can be "hidden" without easy detectability. In the ESD intervals the stored entanglement is not evident either locally or globally. Moreover, these long intervals have two important management characteristics - they have closely predictable durations, and they don't substantially deplete the degree of the stored entanglement.

Finally, we can comment on the quasi-periodic modulations evident in the numeric details in Fig. 5. For contrast, we show in Fig. 6 below the numeric revival details for two other values of coherent state photon num-

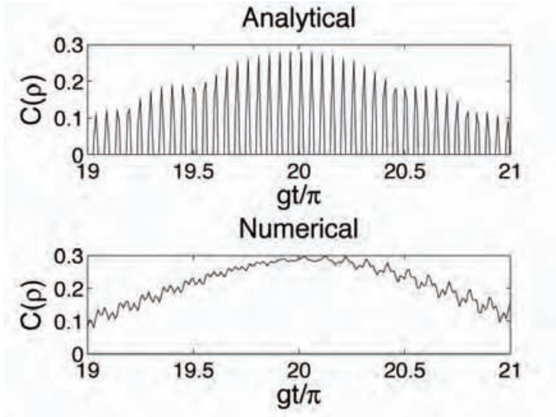

FIG. 5: Details of the first revival shown in the preceding figure. The deep modulations in the analytic envelope are not present in the numerical envelope, which retains entanglement robustly through the revival event.

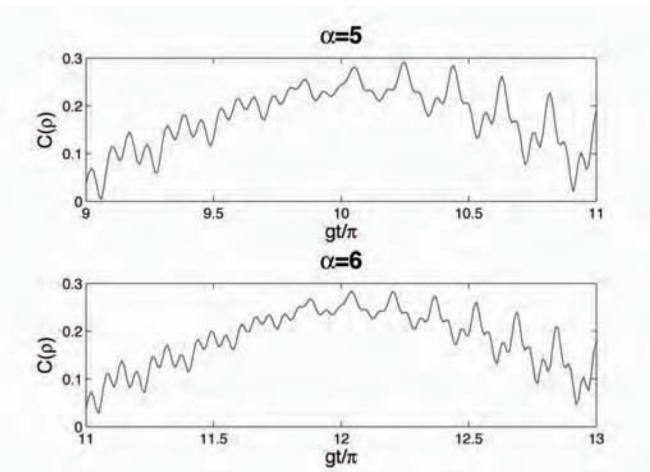

FIG. 6: Similar to Fig. 5 above, except that here $\alpha = 5$ and 6, rather than 10.

.

ber: $\bar{n} = 25$ and 36. In those graphs modulations also appear, but with different main periods, their frequency increasing linearly as α increases, viz., n main modulation periods for $\alpha = n$ over a unit interval in gt/π. These modulations would be further smoothed in realistic applications where differences would have to be expected between the $\bar{n}$ values at the two sites being managed, thus promoting rather than degrading the desirable features mentioned.

VII. ACKNOWLEDGEMENTS

We are pleased to thank Prof. Ting Yu for consultation and collaboration in the early stages of this study. Partial financial support was provided by grants from DARPA HR0011-09-1-0008 and ARO W911NF-09-1-0385.

VIII. APPENDIX

Here, we sketch the saddle point analysis of the remaining sums in Eqn. (60). They can be combined, and converted to an integral:

$$I_{34} \cong \int_0^\infty \exp\left[\alpha^2 f(n)\right] dn, \tag{63}$$

where

$$\begin{aligned} f(n) &= \frac{1}{\alpha^2}\Big(2n\ln\alpha - \frac{1}{2}\ln(2\pi n) \\ &- n\ln(n) + n + 2i\tau\sqrt{n}\Big) - 1. \end{aligned} \tag{64}$$

In the saddle point method, an integral of type $\int_a^b e^{Mf(x)}dx$, where M is a large number and $f(x)$ is a twice-differentiable function, is approximated by,

$$\int_a^b e^{Mf(x)}dx \approx \sqrt{\frac{2\pi}{M|f''(x_0)|}}e^{Mf(x_0)}, \tag{65}$$

where x_0 is the global maximum of $f(x)$. In our application Eq. (63) can be written in this form if we choose $M = \alpha^2$ and $f(n)$ as given above. For the saddle point maximum of $f(n)$ we need to find the point n_0 where $f'(n_0) = 0$:

$$f'(n_0) = \frac{1}{\alpha^2}\Big(2\ln\alpha - \frac{1}{2n_0} - \ln(n_0) + i\tau n_0^{-1/2}\Big) = 0. \tag{66}$$

Assuming that $|n_0|$ is large, we can replace $\ln(n_0) \cong \ln(\alpha^2) + i\tau n_0^{-1/2}$, and then letting $n_0 = \rho e^{i\theta}$ gives

$$\ln\rho + i\theta = \ln(\alpha^2) + i\tau\rho^{-1/2}e^{-i\theta/2}, \tag{67}$$

where equating the real and imaginary parts of both sides gives,

$$\begin{aligned} \ln(\rho) &= \ln(\alpha^2) + \tau\rho^{-1/2}\sin(\theta/2) \\ \theta &= \tau\rho^{-1/2}\cos(\theta/2). \end{aligned} \tag{68}$$

For $\tau = 2\pi k\alpha$, where k is an integer, the equations above become,

$$\rho = \alpha^2 \quad \text{and} \quad \theta = (-1)^k 2\pi k. \tag{69}$$

Now, let $\tau = \tau_0 + \Delta\tau$ and $\theta = \theta_0 + \Delta\theta$, where $\tau_0 = 2\pi k\alpha$ and $\theta_0 = 2\pi k$. Assuming that both $\Delta\tau$ and $\Delta\theta$ are small, we can write

$$\sin(\theta/2) \cong (-1)^k\frac{\Delta\theta}{2} \quad \text{and} \quad \cos(\theta/2) \cong (-1)^k. \tag{70}$$

Then Eq. (68) turns into,

$$\begin{aligned} \rho &\cong \alpha^2[1 + (-1)^k\pi k\Delta\theta] \\ \theta &\cong \theta_0 - \frac{\pi k\Delta\theta}{2} + (-1)^k\frac{\Delta\tau}{\alpha}. \end{aligned} \tag{71}$$

In order to arrive at the second line we have used,

$$\rho^{-1/2} \cong \alpha^{-1}\Big(1-(-1)^k\frac{\pi k\Delta\theta}{2}\Big), \tag{72}$$

in the second line of Eq. (68) and we have ignored the terms with $\Delta\tau\Delta\theta$.

Now, the last two terms in the second line of Eq. (71) are just $\Delta\theta$, so,

$$-\frac{\pi k\Delta\theta}{2}+(-1)^k\frac{\Delta\tau}{\alpha}=\Delta\theta. \tag{73}$$

Thus, we have,

$$\Delta\theta=\frac{(-1)^k}{\alpha(1+\pi^2k^2)}\Delta\tau, \tag{74}$$

Using this in Eq. (71), we obtain

$$\begin{aligned}\rho &\cong \alpha^2[1+\pi k\frac{1}{\alpha(1+\pi^2k^2)}\Delta\tau]\\ \theta &= \theta_0+(-1)^k\frac{1}{\alpha(1+\pi^2k^2)}\Delta\tau.\end{aligned} \tag{75}$$

Now, by inserting $n_0=\rho e^{i\theta}$ in Eq. (89), we find

$$\begin{aligned}\alpha^2 f(n_0) &= -\rho e^{i\theta}\ln(\rho/\alpha^2)-\ln(\rho^{1/2})-\frac{i\theta}{2}\\ &\quad \rho e^{i\theta}(1-i\theta)+2i\tau\rho^{1/2}e^{i\theta/2}\\ &- \alpha^2-\ln(\sqrt{2\pi}).\end{aligned} \tag{76}$$

The real part of this equation is given by,

$$\begin{aligned}Re\{\alpha^2 f(n_0)\} &= -\rho\cos\theta\ln(\rho/\alpha^2)-\ln(\rho^{1/2})+\rho\theta\sin\theta\\ &\quad +\rho\cos\theta-2\tau\rho^{1/2}\sin(\theta/2)\\ &\quad -\alpha^2-\ln(\sqrt{2\pi}).\end{aligned} \tag{77}$$

Using $\theta=\theta_0+\Delta\theta$ and retaining only the terms upto the second order in $\Delta\theta$,

$$\begin{aligned}&Re\{\alpha^2 f(n_0)\}\cong-\rho\Big[1-\frac{(\Delta\theta)^2}{2}\Big]\ln\Big(\frac{\rho}{\alpha^2}\Big)\\ &-\ln(\rho^{1/2})+\rho\Delta\theta(\theta_0+\Delta\theta)+\rho\Big[1-\frac{(\Delta\theta)^2}{2}\Big]\\ &-(-1)^k\tau\rho^{1/2}\Delta\theta-\alpha^2-\ln(\sqrt{2\pi}).\end{aligned} \tag{78}$$

Writing $\Delta\theta$ in terms of $\Delta\tau$ and ignoring the terms after second order,

$$\begin{aligned}&Re\{\alpha^2 f(n_0)\}\cong-\frac{1}{1+\pi^2k^2}\Big(\frac{1+2\pi^2k^2}{2+2\pi^2k^2}\Big)(\Delta\tau)^2\\ &-\ln(\rho^{1/2})-\ln(\rho^{1/2})-\ln(\alpha^{1/2})-\ln(\sqrt{2\pi}).\end{aligned} \tag{79}$$

The imaginary part of $\alpha^2 f(n_0)$ is,

$$\begin{aligned}&Im\{\alpha^2 f(n_0)\}=-\sin\theta\rho\ln(\rho/\alpha^2)-\theta/2\\ &-\rho\theta\cos\theta+\rho\sin\theta+2\tau\rho^{1/2}\cos(\theta/2).\end{aligned} \tag{80}$$

Again, using $\theta=\theta_0+\Delta\theta$ and $\tau=\tau_0+\Delta\tau$, writing $\Delta\theta$ in terms of $\Delta\tau$ and ignoring the terms after second order,

$$\begin{aligned}&Im\{\alpha^2 f(n_0)\}\cong(-1)^k\Big\{2\pi k\alpha^2+\Big[2\alpha\\ &-\frac{1}{2\alpha(1+\pi^2k^2)}\Big]\Delta\tau\\ &+\frac{\pi k}{1+\pi^2k^2}\Big[\frac{3}{2(1+\pi^2k^2)}-\frac{1}{\alpha^2}\Big](\Delta\tau)^2.\end{aligned} \tag{81}$$

For $k=0$ the $(\Delta\tau)^2$ part of this equation vanishes. For $k=1,2,...$ this part can be ignored as well. Thus we are left with,

$$Im\{\alpha^2 f(n_0)\}\cong(-1)^k(2\pi k\alpha^2+2\alpha\Delta\tau). \tag{82}$$

We also need to calculate $\sqrt{2\pi/\alpha^2|f''(n_0)|}$. By using Eq. (66), we find

$$f''(n_0)=\frac{1}{\alpha^2}\Big(\frac{1}{2n_0^2}-\frac{1}{n_0}-\frac{i\tau n_0^{-3/2}}{2}\Big), \tag{83}$$

which has two forms: for $\tau=0$,

$$\sqrt{\frac{2\pi}{\alpha^2|f''(n_0)|}}\cong\sqrt{2\pi}\alpha, \tag{84}$$

and for $\tau=2\pi k\alpha$ (k=1,2,...):

$$\sqrt{\frac{2\pi}{\alpha^2|f''(n_0)|}}\cong\sqrt{\frac{2\pi\alpha}{\pi k}}. \tag{85}$$

Then the integral in Eq. (63) is given by,

$$I_{34}\cong\sqrt{\frac{2\pi}{\alpha^2|f''(n_0)|}}e^{\alpha^2 f(n_0)}. \tag{86}$$

In order to find the value of this integral we should add the contributions from all $k=0,1,2,....$ As a result, the integral is,

$$\begin{aligned}I_{34} &\cong e^{-\tau^2/2}e^{2i\alpha\tau}\\ &\quad+\sum_{k=1,2,...}\sqrt{\frac{1}{\pi k}}\exp\Big[-\frac{(\tau-2\pi k\alpha)^2}{1+\pi^2k^2}\Big]\\ &\quad\times\ \cos[2\alpha(\tau-2\pi k\alpha)].\end{aligned} \tag{87}$$

Now, inserting the values of all four integrals into Eq. (55),

$$\begin{aligned}z-\sqrt{ad} &\cong \frac{1}{4}\Big\{\exp\Big(-\frac{\tau^2}{16\alpha^4}\Big)-1+e^{-\tau^2}\cos(4\alpha\tau)\\ &\quad+\frac{2}{\pi}\sum_{k=1,2,...}\frac{1}{k}\Big[\exp\Big(-\frac{2(\tau-2\pi k\alpha)^2}{1+\pi^2k^2}\Big)\\ &\quad\times\ \cos[4\alpha(\tau-2\pi k\alpha)]\Big]\Big\}.\end{aligned} \tag{88}$$

Writing this last equation we have used the fact that around $\tau=2\pi k\alpha$ only the term with the corresponding

k gives a significant contribution to the squares of the sums in Eq. (55). The contribution to $\tau = 2\pi k\alpha$ from any other k' is proportional to $\exp(-4\pi^2\alpha^2(k-k')^2/[1+\pi^2(k')^2])$, so it decays exponentially with the distance from the peaks identified with integer k. Thus, while taking the squares in Eq. (55) we can ignore the cross-terms.

Now, we turn to the integral given in Eq. (58). We will continue to use the saddle point method. This time we need to find the maximum of the function:

$$\begin{aligned} f(n) &= \frac{1}{\alpha^2}(2n\ln(\alpha) - \frac{1}{2}\ln(2\pi n) \\ &\quad -n\ln(n) + n + \frac{i\tau}{2\sqrt{n}}) - 1, \end{aligned} \tag{89}$$

For this, we need to find the point n_0 where $f'(n_0) = 0$:

$$f'(n_0) = \frac{1}{\alpha^2}(\ln(\alpha^2) - \frac{1}{2n_0} - \ln(n_0) - \frac{i\tau}{4}n_0^{-3/2}) = 0, \tag{90}$$

Again assuming that $|n_0| >> 1$,

$$\ln(n_0) \cong \ln(\alpha^2) - \frac{i\tau}{4}n_0^{-3/2}. \tag{91}$$

Letting

$$n_0 = \rho e^{i\theta}, \tag{92}$$

then,

$$\ln(\rho) + i\theta = \ln(\alpha^2) - \frac{i\tau}{4}\rho^{-3/2}[\cos(\frac{3\theta}{2}) - i\sin(\frac{3\theta}{2})], \tag{93}$$

and by matching the real and imaginary parts of both sides, we find two coupled transcendental equations:

$$\begin{aligned} \ln(\rho) &= \ln(\alpha^2) - \frac{\tau}{4}\rho^{-3/2}\sin(\frac{3\theta}{2}), \\ \theta &= -\frac{\tau}{4}\rho^{-3/2}\cos(\frac{3\theta}{2}). \end{aligned} \tag{94}$$

We are going to retain only the terms up to second order in $\tau\rho^{-3/2}$,

$$\theta \cong -\frac{\tau}{4\alpha^3} \quad \text{and} \quad \rho \cong \alpha^2(1 + \frac{3\theta^2}{2}). \tag{95}$$

With this restriction, and after inserting $n = \rho e^{i\theta}$ into Eq. (89), we find

$$\begin{aligned} \alpha^2 f(n_0) &\cong -ln(\alpha^2) - \ln(\alpha) - \ln(\sqrt{2\pi}) \\ &\quad -\frac{3}{4}\theta^2 - \frac{i\theta}{2} + \rho e^{i\theta}(1 - \frac{3\theta^2}{2} - i\theta) \\ &\quad +\frac{i\tau}{2}\rho^{-1/2}e^{-i\theta/2} - \alpha^2. \end{aligned} \tag{96}$$

Writing ρ in terms of θ and retaining only the terms up to θ^2,

$$\begin{aligned} \alpha^2 f(n_0) &\cong -ln(\alpha^2) - \ln(\alpha) - \ln(\sqrt{2\pi}) \\ &\quad -\frac{3\theta^2}{4} + \frac{\alpha^2\theta^2}{2} + \frac{\tau\theta}{4\alpha} \\ &\quad +i\Big(\frac{\tau}{2\alpha} - \frac{\theta}{2} - \frac{7\tau\theta^2}{16\alpha}\Big), \end{aligned} \tag{97}$$

so that by inserting $-\tau/4\alpha^3$ for θ, we obtain

$$\begin{aligned} \alpha^2 f(n_0) &\cong -ln(\alpha^2) - \ln(\alpha) - \ln(\sqrt{2\pi}) \\ &\quad -\frac{\tau^2}{32\alpha^4} - \frac{3\tau^2}{16\alpha^6} \\ &\quad +i\Big(\frac{\tau}{2\alpha} - \frac{\tau}{8\alpha^3} - \frac{7\tau^3}{256\alpha^7}\Big). \end{aligned} \tag{98}$$

In order to find the final form of Eq. (65) we need to calculate $|f''(n_0)|$ as well.

$$f''(n_0) = \frac{1}{\alpha^2}\Big(\frac{1}{2n_0^2} - \frac{1}{n_0} + \frac{3i\tau}{8}n_0^{-5/2}\Big). \tag{99}$$

Retaining the terms up to α^{-2} in the parentheses, we have $|f''(n_0)| \cong \frac{1}{\alpha^4}$. Then we use Eq. (98) and Eq. (65) and insert α^2 for M, to get

$$\begin{aligned} \sqrt{\frac{2\pi}{\alpha^2|f''(n_0)|}}e^{\alpha^2 f(n_0)} &\cong \exp\Big(-\frac{\tau^2}{32\alpha^4} - \frac{3\tau^2}{16\alpha^6}\Big) \\ &\quad \exp\Big(\frac{i\tau}{2\alpha} - \frac{i\tau}{8\alpha^3} - \frac{7i\tau^3}{256\alpha^7}\Big) \end{aligned} \tag{100}$$

For $\tau \sim \alpha^2$ we can retain the first terms in the parentheses and ignore the rest since $\alpha^2 >> 1$. Thus, we finally find

$$I_{12} \cong \exp\Big(-\frac{\tau^2}{32\alpha^4}\Big)e^{i\tau/2\alpha}. \tag{101}$$

[1] E. Schrödinger, *Naturwiss.* **23**, 807 (1935). See also the closely related paper, A. Einstein, B. Podolsky and N. Rosen, Phys. Rev. **46**, 777 (1935).
[2] M. S. Kim, J. Lee, D. Ahn and P. L. Knight, Phys. Rev. A **65**, 040101(R) (2002).
[3] L. Zhou and G. Yang, J. Phys. B **39**, 5143-5150 (2006).
[4] R. W. Rendell and A. K. Rajagopal, J. Phys. B **67**, 062110 (2006).
[5] E.T. Jaynes and F.W. Cummings, Proc. IEEE **51**, 89 (1963).
[6] G. Rempe, H. Walther and N. Klein, Phys. Rev. Lett. **58**, 353 (1987).
[7] M. Brune *et al.*, Phys. Rev. Lett. **76**, 1800 (1996).
[8] D. M. Meekhof *et al.*, Phys. Rev. Lett. **76**, 1796 (1996).
[9] A. Boca *et al.*, Phys. Rev. Lett **93**, 233603 (2004).
[10] J. Gea-Banacloche, Phys. Rev. Lett. **65**, 3385 (1990).
[11] S.J.D. Phoenix and P.L. Knight, Phys. Rev. A **44**, 6023 (1991).
[12] W.K. Wootters, Phys. Rev. Lett. **80**, 2245 (1998).
[13] T. Yu and J.H. Eberly, Quant. Inf. Comp. **7**, 459 (2007).
[14] T. Yu and J.H. Eberly, J. Mod. Opt. **54**, 2289 (2007).
[15] M. Yönaç, et al., J. Phys. B **39**, S621 (2006), and J. Phys. B **40**, S45 (2007).
[16] I. Sainz and G. Björk, Phys. Rev. A **77**, 052307 (2008).
[17] S. Chan, M. D. Reid and Z. Ficek, J. Phys. B **42**, 065507 (2009).
[18] T. Yu and J.H. Eberly, Science **323**, 598 (2009).
[19] P.J. Dodd and J.J. Halliwell, Phys. Rev. A **69**, 052105 (2004).
[20] J. P. Paz and A. J. Roncaglia, Phys. Rev. Lett. **100**, 220401 (2008).
[21] T. Yu and J.H. Eberly, Phys. Rev. Lett. **97**, 140403 (2006).
[22] M. Yönaç, Ph.D. Thesis, Department of Physics and Astronomy, University of Rochester (2009).
[23] J.H. Eberly, N.B. Narozhny and J.J. Sanchez-Mondragon, Phys. Rev. Lett. **44**, 1323 (1980), and N.B. Narozhny, J.J. Sanchez-Mondragon and J.H. Eberly, Phys. Rev. A **23**, 236 (1981).

Entanglement Evolution in a Non-Markovian Environment

Ting Yu[1*] and J. H. Eberly[2†]
[1] *Center of Controlled Quantum Systems and Department of Physics and Engineering Physics, Stevens Institute of Technology, Hoboken, New Jersey 07030-5991, USA*
[2] *Rochester Theory Center and Department of Physics and Astronomy, University of Rochester, Rochester, New York 14627-0171, USA*
(Dated: September 2, 2009)

We extend recent theoretical studies of entanglement dynamics in the presence of environmental noise, following the long-time interest of Krzysztof Wodkiewicz in the effects of stochastic models of noise on quantum optical coherences. We investigate the quantum entanglement dynamics of two spins in the presence of classical Ornstein-Uhlenbeck noise, obtaining exact solutions for evolution dynamics. We consider how entanglement can be affected by non-Markovian noise, and discuss several limiting cases.

Key words: Entanglement dynamics, Stochastic Schrödinger Equation, Kraus Operators, Master Equations

PACS numbers: 03.65.Yz, 03.65.Ud, 03.67.-a

I. INTRODUCTION

A quantum system of interest may be large or small, but its background, called an environment, is almost always complex, and is often represented by a bath of bosons or fermions, or by classical random fields. In all these cases, system dynamics is described by a quantum master equation that governs the evolution of the reduced density matrix of the system. In the current decade, decoherence dynamics of entangled quantum systems under the influence of environmental noises has been extensively discussed in different contexts involving atoms, ions, photons, quantum dots, and Josephson junctions, to name several. This is all related to new regimes of information processing, such as quantum cryptography and quantum computation [1]. An important category of such research has treated the fascinating domain where entanglement of qubits evolves even though the qubits do not interact, even indirectly. An example is sketched in Fig. 1 and we restrict our attention here to this category.

In experimental environments an entangled system may be exposed to vacuum noise, phase noise, thermal noise, and various classical noises, as well as mixed combinations of noises. A number of idealized models have provided new insights by allowing entanglement evolution to be followed by solving the appropriate quantum master equation (see Zyczkowski, et al. [2], Daffer, et al. [3], as well as [4–9]). Most research on entanglement dynamics has been focused on ambient noises from environments that obey the Markov (no memory) assumption. Recently, there is growing interest in the non-Markovian entanglement dynamics for both discrete and continuous quantum systems (see [10–15] and the overview in [9]).

In truth every environment is non-Markovian. Non-Markovian noise was a repeated theme in the research of Krzysztof Wodkiewicz [16–27], and we present our findings as a contribution to his scientific memory.

As far as we know there are no fully systematic investigations of non-Markovian noises or of their effect on the coherence dynamics of non-interacting spin systems. In particular, a perturbative theory leading to the Markov approximation is still lacking. The purpose of this paper is to present a study of such problems in the simplest form. We will consider classical non-Markovian noises, modelling them as so-called Ornstein-Uhlenbeck processes, and derive the consequences for entanglement dynamics. This can be considered an extension of our earlier note on entanglement sudden death (ESD) under classical Markov noises [28].

II. THE KUBO-ANDERSON MODEL EXTENDED TO TWO QUBITS

We consider an entangled pair of spins both of which are subject to frequency fluctuations that are random [29]. We adopt a model for these fluctuations that

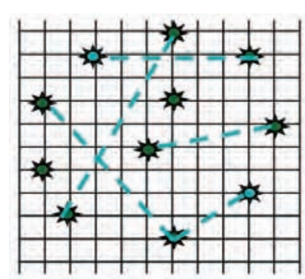

FIG. 1: Sketch of remote qubits in a quantum memory net, where the dashed lines indicate entanglement, but not interaction.

*Email address: ting.yu@stevens.edu
†Email address: eberly@pas.rochester.edu

treats them as caused by noisy environments described by Ornstein-Uhlenbeck processes. This well-known Gaussian noise model is non-Markovian in the general case but has a well-defined Markov limit. To focus exclusively on the effects on the entanglement of the spins as it arises from the noise, we assume the spins to be affected separately by separate environments, and not to interact with each other in any way, especially not through the noises. Thus the spins could be, for example, remote components of a quantum memory net (as in Fig. 1) under steady attack by weak local noise. This compromises the preservation of their entanglement.

The Hamiltonian of the two-spin system can then be formally written as (we set $\hbar = 1$):

$$H_{\rm tot}(t) = \frac{\Omega_A(t)}{2}\sigma_z^A + \frac{\Omega_B(t)}{2}\sigma_z^B \tag{1}$$

where $\Omega_A(t)$ and $\Omega_B(t)$ are the independent fluctuations of the spin transition frequencies (level spacings). They have the mean value properties

$$\begin{aligned} M[\Omega_i(t)] &= 0, \qquad (2)\\ M[\Omega_i(t)\Omega_i(s)] &= \alpha(t-s) \\ &= \frac{\Gamma_i\gamma}{2}e^{-\gamma|t-s|}, \quad i = A, B, \qquad (3)\end{aligned}$$

where $M[\cdot]$ stands for the statistical mean over the noises $\Omega_A(t)$ and $\Omega_B(t)$. Note that γ is the noise bandwidth, and $\gamma^{-1} = \tau_c$ defines the environment's finite correlation time of the noise. For simplicity, we will take the noise properties to be the same for A and B (e.g., $\Gamma_A = \Gamma_B \equiv \Gamma$), although independent. In the limit $\gamma \to \infty$, Ornstein-Uhlenbeck noise reduces to the well-known Markov case:

$$\alpha(t,s) = \Gamma\delta(t-s). \tag{4}$$

For the total system described by the Hamiltonian (1), the stochastic Schrödinger equation is given by

$$i\frac{d}{dt}|\psi(t)\rangle = H_{\rm tot}(t)|\psi(t)\rangle. \tag{5}$$

The explicit solution for the stochastic Schrodinger equation can be readily obtained in terms of a stochastic unitary operator:

$$|\psi(t)\rangle = U(t,\Omega_A,\Omega_B)|\psi(0)\rangle, \tag{6}$$

where the stochastic propagator $U(t,\Omega_A,\Omega_B)$ is given by

$$U(t,\Omega_A,\Omega_B) = e^{-i\int_0^t ds\left(\Omega_A(s)\sigma_z^A + \Omega_B(s)\sigma_z^B\right)}. \tag{7}$$

The reduced density matrix for spins A and B is then obtained from the statistical mean

$$\rho(t) = M[|\psi(t)\rangle\langle\psi(t)|]. \tag{8}$$

The master equation for the reduced density matrix for the two-spin system in a non-Markovian regime can be readily derived from the stochastic Schrödinger equation [30]:

$$\frac{d\rho}{dt} = \frac{G(t)}{4}(2\rho - \sigma_z^A\rho\sigma_z^A - \sigma_z^B\rho\sigma_z^B), \tag{9}$$

where

$$G(t) = \int_0^t \alpha(t-s)ds = \frac{\Gamma}{2}(1-e^{-\gamma t}), \tag{10}$$

The memory information of the environmental noises is encoded in the time-dependent coefficient $G(t)$ where $\tau_c = 1/\gamma$ characterizes the environmental memory time. In the Markov limit $\tau_c \to 0$ ($\gamma \to \infty$), when $G(t) \to \Gamma/2$, equation (9) reduces to the well-known Markov master equation in the presence of dephasing noises.

III. EXACT SOLUTIONS FOR QUANTUM EVOLUTION

Solutions of master equations for the noisy evolution of two-spin density matrices in terms of the Kraus operator-sum-representation have been given before (see, for example, [28, 31, 32]). In many cases of physical interest, the Kraus representation allows a transparent analysis of entanglement decoherence without invoking the explicit forms of the initial conditions. In what follows, we will use the fact that for any two-spin initial state ρ (pure or mixed), the evolution of the reduced density matrix can be written compactly as

$$\rho(t) = \sum_\mu K_\mu(t)\rho(0)K_\mu^\dagger(t), \tag{11}$$

where the Kraus operators K_μ satisfy $\sum_\mu K_\mu^\dagger K_\mu = 1$ for all t.

In order to derive the desired Kraus operators for the reduced density matrix we begin by noting that the solution for just spin A can be written:

$$|\psi(t)\rangle = U(\Omega_A,t)|\psi(0)\rangle \tag{12}$$

where

$$U(\Omega_A,t) = \exp\left[-iF(t)\sigma_z\right] \tag{13}$$

with the stochastic process $F(t) = \int_0^t ds\Omega_A(s)$. Then our first task is to express the stochastic density operator $\rho_{\rm st} = |\psi(t)\rangle\langle\psi(t)|$ in the Kraus-like operator representation form:

$$\rho_{st}(t) = \exp\left[-iF(t)\sigma_z\right]\rho(0)\exp\left[iF(t)\sigma_z\right] \tag{14}$$

where $\rho(0) = |\psi(0)\rangle\langle\psi(0)|$ is the initial state of the system, which is assumed to be independent of the noise. The desired Kraus operators for the spin are obtained by taking a statistical mean over the noise $\Omega_A(t)$ for qubit A and are given by

$$E_1 = \begin{pmatrix} p_A(t) & 0 \\ 0 & 1\end{pmatrix},\ E_2 = \begin{pmatrix} q_A(t) & 0 \\ 0 & 0\end{pmatrix}, \tag{15}$$

where the time-dependent Kraus matrix elements are

$$\begin{aligned} q_A(t) &= \sqrt{1-p_A^2(t)}, \quad \text{and} && (16)\\ p_A(t) &= \exp\left[-f(t)\right], \quad \text{with} && (17)\\ f(t) &\equiv \int_0^t G(s)ds \\ &= \frac{\Gamma}{2}[\, t+\frac{1}{\gamma}(e^{-\gamma t}-1)\,], && (18)\end{aligned}$$

and similar expressions for $p_B(t)$ and $q_B(t)$. The two-qubit case given here can be easily applied to N noninteracting qubits, an extension we reserve for later attention.

Since our two spins are evolving independently, we have the following four Kraus operators in terms of the tensor products of E_1 and E_2:

$$\begin{aligned} K_1 &= \begin{pmatrix} p_A & 0\\ 0 & 1\end{pmatrix} \otimes \begin{pmatrix} p_B & 0\\ 0 & 1\end{pmatrix}, && (19)\\ K_2 &= \begin{pmatrix} p_A & 0\\ 0 & 1\end{pmatrix} \otimes \begin{pmatrix} q_B & 0\\ 0 & 0\end{pmatrix}, && (20)\\ K_3 &= \begin{pmatrix} q_A & 0\\ 0 & 0\end{pmatrix} \otimes \begin{pmatrix} p_B & 0\\ 0 & 1\end{pmatrix}, && (21)\\ K_4 &= \begin{pmatrix} q_A & 0\\ 0 & 0\end{pmatrix} \otimes \begin{pmatrix} q_B & 0\\ 0 & 0\end{pmatrix}. && (22)\end{aligned}$$

IV. NON-MARKOVIAN ENTANGLEMENT DYNAMICS

A. X matrix and concurrence

We now consider entanglement dynamics of two half-integral spins (qubits) with an initial density matrix with the common X-form [31]:

$$\rho^{AB} = \begin{pmatrix} \rho_{11} & 0 & 0 & \rho_{14}\\ 0 & \rho_{22} & \rho_{23} & 0\\ 0 & \rho_{32} & \rho_{33} & 0\\ \rho_{41} & 0 & 0 & \rho_{44}\end{pmatrix}. \qquad (23)$$

Such X states occur in many contexts and include pure Bell states as well as Werner mixed states.

For two qubits, entanglement can be evaluated unambiguously via the concurrence function [33], which may be calculated explicitly from the density matrix ρ^{AB}. For qubits A and B we have: $C^{AB} = C(\rho^{AB}) = \max\{0, Q(t)\}$. Here $Q(t)$ is defined as

$$Q = \sqrt{\lambda_1} - \sqrt{\lambda_2} - \sqrt{\lambda_3} - \sqrt{\lambda_4}, \qquad (24)$$

where the quantities λ_i are the (generally time-dependent) eigenvalues in decreasing order of the following (nonlinear in ρ) matrix:

$$\zeta = \rho(\sigma_y^A \otimes \sigma_y^B)\rho^*(\sigma_y^A \otimes \sigma_y^B), \qquad (25)$$

where ρ^* denotes the complex conjugation of ρ in the standard basis $|+,+\rangle, |+,-\rangle, |-,+\rangle, |-,-\rangle$, and σ_y is the usual Pauli matrix expressed in the same basis.

From the general solution (19-22), one can easily show for the initial state (23) that one finds

$$\begin{aligned} Q(t) &= 2\max\Big(|\rho_{32}(t)| - \sqrt{\rho_{11}(0)\rho_{44}(0)}, \\ &\qquad |\rho_{14}(t)| - \sqrt{\rho_{22}(0)\rho_{33}(0)}\Big). && (26)\end{aligned}$$

B. Solutions for non-Markovian disentanglement

The Ornstein-Uhlenbeck phase-noise solutions for the density matrix elements of a general initial state are given by

$$\begin{aligned} \rho_{12}(t) &= \rho_{12}(0)e^{-f(t)}, && (27)\\ \rho_{13}(t) &= \rho_{13}(0)e^{-f(t)}, && (28)\\ \rho_{24}(t) &= \rho_{24}(0)e^{-f(t)}, && (29)\\ \rho_{34}(t) &= \rho_{34}(0)e^{-f(t)} && (30)\\ \rho_{23}(t) &= \rho_{23}(0)e^{-2f(t)}, && (31)\\ \rho_{14}(t) &= \rho_{14}(0)e^{-2f(t)} && (32)\\ \rho_{ii}(t) &= \rho_{ii}(0) \ \ (i=1,2,3,4) && (33)\end{aligned}$$

where $f(t)$ is defined in (18). Let us note that in the limit $\gamma \to \infty$, we recover the standard Markov approximation where $f(t) = \Gamma t/2$.

Although there is no compact analytical expression for the concurrence $C(\rho(t))$ with an arbitrary initial state, we can readily show that preservation of entanglement is restricted by the inequality

$$C(\rho(t)) \le e^{-2f(t)}C(\rho(0)). \qquad (34)$$

A sharper result occurs for the X matrix under consideration because the diagonal elements are independent of t. Since they all vanish as $\exp(-f(t))$ for increasing t, we know that $Q(t)$ must eventually become strictly negative if diagonal values are initially non-zero (e.g., any finite-temperature equilibrium state). Negative Q mandates $C^{AB} = 0$, so ESD must occur. Next we will consider key limiting cases.

C. Entanglement decay: Stationary limit

We consider now the stationary limit $\gamma t \gg 1$. Then

$$f(t) = \frac{\Gamma}{2}[t + \frac{1}{\gamma}(e^{-\gamma t} - 1)] \to \frac{\Gamma}{2}t \qquad (35)$$

Therefore, from (34), we get

$$C(\rho(t)) \le e^{-\Gamma t}C(\rho(0)). \qquad (36)$$

Hence, the entanglement decay rate is at least as rapid as Γ, and may be much faster. Clearly, the stationary limit is identical to the Markov limit $\alpha(t-s) = \Gamma\delta(t-s)$.

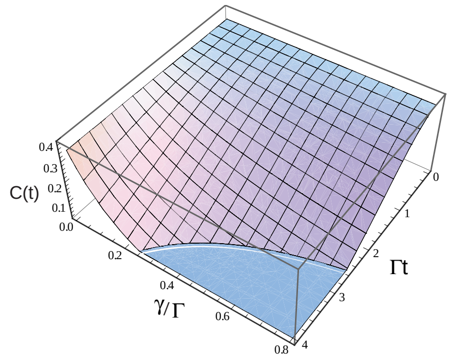

FIG. 2: The graph shows C^{AB} vs. Γt and γ/Γ. The value $\alpha = 1/3$ has been chosen. The reservoir bandwidth γ controls the approach to the Markov limit, and we see that for $\gamma < \Gamma$ the inevitable onset of ESD (the region where $C(t) = 0$) can be substantially delayed.

D. Entanglement decay: Short-time limit

Now let us turn to the opposite limiting case: $\gamma t \ll 1$. In this case, we can use the following approximation,

$$e^{-\gamma t} \sim 1 - \gamma t + \frac{1}{2}\gamma^2 t^2 \tag{37}$$

Therefore,

$$f(t) = \frac{1}{4}\Gamma\gamma t^2 \tag{38}$$

Then concurrence decay is bounded by

$$C(\rho(t)) \leq e^{-\frac{1}{2}\Gamma\gamma t^2} C(\rho(0)) \tag{39}$$

Hence, the effective disentanglement time is given by:

$$\tau_{\text{dis}} = \sqrt{\frac{2}{\Gamma\gamma}} \tag{40}$$

Clearly, for non-Markovian noises, the short-time limit is more interesting since it shows that the resultant entanglement behavior deviates significantly from the well-known Markov dynamics. Obviously, the smaller γ is, the better approximation we have. For both limiting cases, it is easy to prove that a sufficient condition for ESD to occur is $\rho_{11}\rho_{22}\rho_{33}\rho_{44} \neq 0$ [34].

V. EVALUATION FOR A SPECIAL X STATE

In Fig. 2 we show the evolution of the concurrence for a specific X-form entangled state:

$$\rho_\alpha^{AB}(0) = \frac{1}{3}\begin{pmatrix} \alpha & 0 & 0 & 0 \\ 0 & 1 & 1 & 0 \\ 0 & 1 & 1 & 0 \\ 0 & 0 & 0 & 1-\alpha \end{pmatrix}, \tag{41}$$

where $0 \leq \alpha \leq 1$, so the initial concurrence is $C(0) = 2/3[1 - \sqrt{\alpha(1-\alpha)}] > 0$.

The time dependence of the concurrence of this state is well-known in the Markov dephasing limit [9, 28]. For our present non-Markovian case, which introduces the environmental bandwidth γ, the time dependence of the Q parameter satisfies

$$Q(t) = \frac{2}{3}\left(e^{-f(t)} - \sqrt{\alpha(1-\alpha)}\right). \tag{42}$$

For all finite values of γ the quantity $e^{-f(t)}$ approaches zero exponentially at long times, and then $Q(t)$ must become negative, so ESD inevitably occurs, with a finite disentanglement time t_{ESD} given by

$$e^{-2f(t_{\text{ESD}})} = \alpha(1-\alpha). \tag{43}$$

Fig. 3 shows several interesting features of entanglement evolution under Ornstein-Uhlenbeck noise. Clearly, we see that non-Markovian noises have markedly different affects on entanglement evolution at short times, while the long time limit gives rise to familiar Markov behavior. First, note that ESD must occur for the entire parameter range of α, except for the end points $\alpha = 0, 1$, given our initial X-state. However, the ESD times are different for non-Markovian short-time and stationary limit

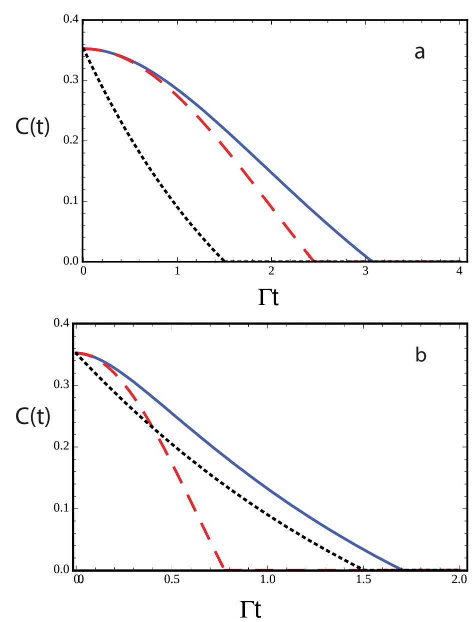

FIG. 3: The graphs show C_α^{AB} vs. t with $\alpha = 1/3$. Fig. 3a shows that with $\gamma/\Gamma = 0.5$, an initially non-Markovian entanglement (solid line) evolves in a markedly different way compared to its Markov limit (dotted line). Clearly, the short-time limit (dashed line) gives a better approximation than the stationary limit (dotted line). However, as shown in Fig.3b where $\gamma/\Gamma = 5$, the difference is washed out at later times when the short-time limit (dashed line) ceases to be a good approximation.

cases. From Fig. 3a, it should be noted that the disentanglement time for non-Markovian regimes could be significantly longer than the disentanglement times in the Markov limit if the dissipation is small. However, once the state becomes separable it will never become entangled again. That is, entanglement rebirth or revival does not occur for Ornstein-Uhlenbeck noise [14].

VI. CONCLUDING REMARKS

We have presented here, as a contribution to the scientific memory of Krzystof Wodkiewicz, the first results of a new investigation that has clear connections to his long-time interest in quantum systems evolving under the influence of stochastic perturbations. One of the targets of his creativity and energy, over many years, was the challenge presented by the influence of non-Markovian noise and we have addressed that challenge with some calculations focused on entanglement.

We have shown that entanglement dynamics under Ornstein-Uhlenbeck noise can be affected in several different ways, depending on the initial entangled states and the noise correlation time. It can be seen that the non-Markovian properties can prolong the life of entanglement. We note that the effective long-time relaxation rate Γ is ordinarily associated with experimentally accessible relaxation times such as T_1 and T_2. Fig. 2 highlights the unusual domain $\gamma < \Gamma$, in which these times are shorter than the internal environmental relaxation time τ_c. Entanglement survival is of fundamental interest at short times in quantum information processing (see [35, 36]). In the case of the short-time limit our results capture the features of quadratic rather than exponential decay at early times. In this simple model, non-Markovian noises appear to play a role as a short-time decoherence buffer, but entanglement measured by concurrence will inevitably conform to the stationary limit at long times. Finally, it is interesting to note that our findings based on the classical phase noise model can be extended into the case of quantum phase noises where the environment is modeled as a set of harmonic oscillators at a finite temperature [37].

Acknowledgements

TY and JHE acknowledge partial financial support from the following agencies: DARPA HR0011-09-1-0008, ARO 48422-PH, NSF PHY-0601804, NSF PHY-0925174.

[1] R. Horodecki, P. Horodecki, M. Horodecki and K. Horodecki, Rev. Mod. Phys. **81**, 865(2009).
[2] K. Zyczkowski, et al. Phys. Rev. A **65**, 012101 (2001).
[3] S. Daffer, K. Wodkiewicz and J. K. McIver, Phys. Rev. A **67**, 062312 (2003).
[4] T. Yu and J. H. Eberly, Phys. Rev. Lett. **93**, 140404 (2004).
[5] T. Yu and J. H. Eberly, Phys. Rev. Lett. **97**, 140403 (2006).
[6] F. Mintert, A. R. R. Carvalho, M. Kus, and A. Buchleitner, Phys. Rep. **415**, 207 (2005).
[7] M. P. Almeida et al, Science **316**, 579 (2007).
[8] J. H. Eberly and T. Yu, Science **316**, 555 (2007).
[9] T. Yu and J.H. Eberly, Science **323**, 598 (2009), and references therein.
[10] B. Bellomo, R. Lo Franco, G. Compagno, Phys. Rev. Lett. **99**, 160502 (2007).
[11] J. P. Paz and A. J. Roncaglia, Phys. Rev. Lett. **100**, 220401 (2008).
[12] J. Dajka, M. Mierzejewski and J. Luczka, Phys. Rev. A **77**, 042316 (2008).
[13] X. F. Cao and H. Zheng, Phys. Rev. A **77**, 022320 (2008).
[14] For recent experimental research involving non-Markovian entanglement dynamics, see J. S. Xu et al, arXiv:0903.5233.
[15] C. Anastopoulos, S. Shresta, and B. L. Hu, arXiv: quant-ph/0610007.
[16] K. Wodkiewicz and J.H. Eberly, Markovian and non-Markovian behavior in 2-level atom fluorescence, Ann. Phys. **101**, 574-593 (1976).
[17] K. Wodkiewicz, Non-Markovian resonance fluorescence, Phys. Lett. A **73**, 94-96 (1979).
[18] K. Wodkiewicz, Functional representation of a non-Markovian probability-distribution in statistical-mechanics, Phys. Lett. A **84**, 56-58 (1981).
[19] K. Wodkiewicz, Langevin-equations with colored noise in quantum optics, Acta Phys. Pol. A **63**, 191-200 (1983).
[20] J. H. Eberly, K. Wodkiewicz and B. W. Shore, Noise in strong laser-atom interactions - phase telegraph noise, Phys. Rev. A **30**, 2381-2389 (1984).
[21] K. Wodkiewicz, B. W. Shore and J. H. Eberly, Noise in strong laser-atom interactions - frequency fluctuations and nonexponential correlations, Phys. Rev. A **30**, 2390-2398 (1984).
[22] K. Wodkiewicz, B. W. Shore and J. H. Eberly, Pre-Gaussian Noise In Strong Laser Atom Interactions, J. Opt. Soc. Am. B **1**, 398-405, (1984).
[23] K. Wodkiewicz, J. H. Eberly and B. W. Shore, Phase and frequency jump theory of laser band shape, J. Opt. Soc. Am. 1, 506-506 (1984).
[24] K. Wodkiewicz and J. H. Eberly, Shot noise and general jump-processes in strong laser-atom interactions, Phys. Rev. A **31**, 2314-2317 (1985).
[25] K. Wodkiewicz, Spontaneous and induced emission of soft bosons - Exact non-Markovian solution - Comment, Phys. Rev. Lett. **63**, 2693-2693 (1989).
[26] M. Kus, E. Wajnryb and K. Wodkiewicz, Mean 1st-passage time in the presence of colored noise - a random-telegraph-signal approach, Phys. Rev. A **43**, 4167-4174 (1991).
[27] M. Kus and K. Wodkiewicz, Mean 1st-passage time in the presence of telegraph noise and the Ornstein-Uhlenbeck process, Phys. Rev. E **47**, 4055-4063 (1993).

[28] T. Yu and J. H. Eberly, Opt. Commun. **264**, 393 (2006).
[29] R. Kubo, M. Toda, and N. Hashitsume, *Statistical Physics II*, (Berlin, Springer, 1991).
[30] W. Strunz and T. Yu, Phys. Rev. A **69**, 052115 (2004); and T. Yu, Phys. Rev. A **69**, 062107 (2004).
[31] T. Yu and J. H. Eberly, Quant. Inf. and Comp. **7**, 459 (2007).
[32] T. Yu and J. H. Eberly, Phys. Rev. B **68**, 165322 (2003).
[33] W. K. Wootters, Phys. Rev. Lett. **80**, 2245 (1998).
[34] J. H. Huang and S. Y. Zhu, Phys. Rev. A **76**, 062322 (2007) and Opt. Commun. **281**, 2156 (2008).
[35] D. Gordon, Euro. Phys. Lett. **83**, 30009 (2008).
[36] J. H. An, Y. Yeo and W. M. Zhang, J. Phys. A **42**, 015302 (2009).
[37] T. Yu and J. H. Eberly, Phys. Rev. B **66**, 193306 (2002).